Transcriptional and translational adaptation to aerobic nitrate anabolism in the denitrifier *Paracoccus denitrificans*

Victor M. Luque-Almagro[1], Isabel Manso[1], Matthew J. Sullivan[2], Gary Rowley[2], Stuart J. Ferguson[3], Conrado Moreno-Vivián[1], David J. Richardson[2] Andrew J. Gates[2], M. Dolores Roldán[1*]

[1]*Departamento de Bioquímica y Biología Molecular, Universidad de Córdoba, Edificio Severo Ochoa, 1ª planta, Campus de Rabanales, Córdoba, 14071, Spain.*
[2]*School of Biological Sciences, University of East Anglia, Norwich Research Park, Norwich, NR4 7TJ, UK.*
[3]*Department of Biochemistry, University of Oxford, South Parks Road, Oxford, OX1 3QU, UK.*

∗ Corresponding author address:
Departamento de Bioquímica y Biología Molecular
Universidad de Córdoba
Córdoba 14071
Spain
Tel: +34 957218318
Fax: +34 957218592
E-mail: bb2rorum@uco.es

Running title: Regulation of nitrate and nitrite assimilation in *Paracoccus denitrificans*

Keywords: Global nitrogen regulator Ntr, nitrate assimilation, nitrate reductase, nitrate/nitrite sensor protein, nitrogen regulation, *Paracoccus.*

SUMMARY STATEMENT

Transcriptomic, proteomic and mutational analyses of the nitrate assimilatory system in *P. denitrificans* PD1222 reveals that nitrate exerts a very tight regulation at the transcriptional and translational levels through the NtrBC and the NasTS systems.

AUTHOR CONTRIBUTION

Matthew J. Sullivan (MJS) and Gary Rowley (GR) contributed to the microarray construction under the supervision of David J. Richardson (DJR), Stuart J. Ferguson (SJF) and Andrew J. Gates (AJG). Proteomic analysis and generation of mutant strains were carried out by Victor M. Luque-Almagro (VLA) under the supervision of Conrado Moreno-Vivián (CMV) and M. Dolores Roldán (MDR). RT-PCR and qPCR was performed by Isabel Manso (IM) under the supervision of CMV, MDR and AJG. The final version of this manuscript has been written by MDR and discussed and revised in agreement with DJR, CMV and SJF.

ABSTRACT

Transcriptional adaptation to nitrate-dependent anabolism by *Paracoccus denitrificans* PD1222 was studied. A total of 74 genes were induced in cells grown with nitrate as N-source compared to ammonium, including *nasTSABGHC* and *ntrBC* genes. The *nasT* and *nasS* genes were cotranscribed, although *nasT* was more strongly induced by nitrate than *nasS*. The *nasABGHC* genes constituted a transcriptional unit, which is preceded by a non-coding region containing hairpin structures involved in transcription termination. The *nasTS* and *nasABGHC* transcripts were detected at similar levels with nitrate or glutamate as N-source, but *nasABGHC* transcript was undetectable in ammonium-grown cells. The nitrite reductase NasG subunit was detected by 2D-PAGE in cytoplasmic fractions from nitrate-grown cells, but it was not present when either ammonium or glutamate was used as N-source. The *nasT* mutant lacked both *nasABGHC* transcript and NADH-dependent nitrate reductase activity. On the contrary, the *nasS* mutant showed similar levels of the *nasABGHC* transcript to the wild-type strain and displayed NasG protein and NADH-nitrate reductase activity with all N-sources tested, except with ammonium. Ammonium repression of *nasABGHC* was dependent on the Ntr system. The *ntrBC* and *ntrYX* genes were expressed at low levels regardless of the nitrogen source supporting growth. Mutational analysis of the *ntrBCYX* genes indicated that while *ntrBC* genes are required for nitrate assimilation, *ntrYX* genes can only partially restore growth on nitrate in absence of *ntrBC* genes. The existence of a regulation mechanism for nitrate assimilation in *P. denitrificans*, by which nitrate induction operates at both transcriptional and translational levels, is proposed.

INTRODUCTION

The soil denitrifier *Paracoccus denitrificans* PD1222 makes multiple metabolic uses of nitrate: (i) as a respiratory electron acceptor to support anaerobic growth, catalysed by a membrane-bound nitrate reductase (Nar); (ii) as an electron sink to dispose of excess reductant during aerobic metabolism of highly reduced carbon substrates, catalysed by the periplasmic nitrate reductase (Nap); and (iii) as nitrogen source for anabolism during both oxic and anoxic growth. The first two processes have been widely studied [1], but the biochemistry and regulation of the third process, nitrate assimilation, has received much less attention. The nitrate assimilation system (Nas) is encoded by the *nasABGHC* gene cluster, which contains a nitrate transporter (NasA), an NADH-dependent nitrite reductase (NasB), a small Rieske-type protein required for both nitrate and nitrite reduction (NasG), a nitrite transporter (NasH), and a nitrate reductase (NasC), which receives electrons from NADH *via* NasB and NasG [2]. The NasB and NasG proteins are essential for growth with nitrate or nitrite as sole nitrogen source under both aerobic and anaerobic conditions. However, the NasA and NasC proteins are required for nitrate import and reduction only under aerobic conditions because of a functional overlap with biochemical components of the respiratory nitrate reductase system that are synthesised under anaerobic conditions [2,3].

Nitrate assimilation is regulated in response to nitrate by a two-component system, encoded by the *nasTS* genes, which are located directly upstream from the *nasA* gene. NasS acts as nitrate/nitrite sensor whereas NasT has an ANTAR (AmiR and NasR transcription antitermination regulators) domain for acting as a transcriptional antiterminator [4,5]. In the absence of nitrate or nitrite, NasS and NasT form an inactive tetrameric complex (two units of each), leading to the premature termination of the *nasABGHC* gene transcription. In the presence of nitrate or nitrite, the NasTS complex becomes dissociated, and thereby NasT allows expression of *nas* genes [5]. Recently, the *P. dentrificans* PD1222 whole genome has been analyzed by using the Quadparser programme, revealing the existence of a guanine-rich region located upstream of the *nasT* gene that forms a canonical G-quadruplex structure. Stabilization of this secondary structure in DNA has been suggested to act as a negative regulator for nitrate-dependent growth [6].

Nitrate assimilation is a widespread metabolic capacity in proteobacteria that usually is controlled at the transcriptional level by nitrate and nitrite induction and by ammonium repression [7,8]. In cyanobacteria, the catabolite activator protein (CAP) family transcription factor NtcA represses the nitrate reductase genes in the presence of ammonium, whereas it activates transcription of these genes at a high C/N ratio (nitrogen depletion), reflected by high 2-oxoglutarate levels [9-11]. In some cyanobacteria, the LysR family transcription regulator NtcB is required for the nitrate/nitrite-dependent induction of the nitrate reductase gene [11]. In Gram positive bacteria like *Bacillus subtilis* and *Streptomyces coelicolor* the TnrA and GlnR regulators respond to nitrogen starvation [12,13]. In *Klebsiella oxytoca*, expression of the nitrate assimilation genes is activated under low nitrogen conditions through the global nitrogen regulatory Ntr system, including NtrA, NtrB and NtrC proteins, and by nitrate/nitrite induction through NasR, a transcription antitermination protein that also binds to nitrate [14,15]. The crystal structure of the *Klebsiella oxytoca* NasR protein has been solved; it is a dimer with a large N-terminal nitrate and nitrite-sensor (NIT) domain and a C-terminal ANTAR domain necessary for specific binding to leader

mRNA. The NIT domain binds nitrate and nitrite between two conserved arginine residues located on adjacent helices [16]. In *Azotobacter vinelandii* and *Pseudomonas putida*, as well as in *P. denitrificans*, two different proteins NasT and NasS act as transcriptional antiterminator and nitrate sensor, respectively [17-20].

The NtrBC two-component system has been extensively characterized in enteric bacteria [21]. NtrB is a sensor kinase that autophosphorylates on a histidine residue under low nitrogen concentrations and transfers a phosphoryl group to the NtrC response regulator protein on a specific aspartate residue [22]. Phosphorylated NtrC acts as a transcriptional activator that oligomerizes on the DNA template with ATPase activity [23]. The NtrC members are usually dependent on the σ^{54} factor (NtrA) and they are involved in transcription of genes related to nitrogen metabolism, such as the glutamine synthetase *glnA* gene. However, in *Rhodobacter capsulatus* a regulatory two-component NtrBC system has been described in which the NtrC component is not σ^{54}-dependent to activate transcription of *nifA1* and *nifA2* genes, which code for transcriptional activators that induce nitrogen fixation gene expression, and the *glnB* gene that is a negative regulator of the *R. capsulatus* NtrBC system under nitrogen excess [24].

The NtrYX system is also a two-component regulatory system with similarity to the sensor/kinase NtrB and the regulatory protein NtrC, respectively. This system has been investigated in diazotrophs with a proposed role in nitrogen assimilation. In *Azorhizobium caulinodans*, a mutant in the *ntrX* gene was found to be defective in using nitrate as nitrogen source, and showed also a reduced *nifA* expression under nitrogen fixation conditions with a disturbed symbiotic phenotype. In the *ntrC* mutant strain, expression of the *ntrYX* operon was derepressed in the presence of nitrate, suggesting an interaction between both NtrBC and NtrYX systems [25]. The NtrBC system in *Azospirillum brasilense* is involved in regulation of nitrate assimilation, ammonium transport, and nitrogenase switch-off by ammonium. The NtrYX system may be involved in nitrate utilization through a possible substitution of the NtrBC system by the NtrYX sensor-regulator pair [26,27]. *Herbaspirillum seropedicae* is a diazotrophic β-proteobacterium with both NtrBC and NtrYX systems displaying a role in regulation of nitrate assimilation [28]. The photosynthetic bacterium *Rhodobacter capsulatus* also has both NtrBC and NtrYX systems, with a function of the NtrBC system in urea assimilation and nitrogen fixation, but with an unclear physiological function of the NtrYX system [29]. The NtrYX system of *Brucella* spp. is involved in redox sensing and regulation of denitrification genes. Expression of *narGHIJK*, *nirKV*, *norBCDEFQ* and *nosDFLRXYZ* genes are down-regulated in an *ntrY* mutant strain under aerobic and microaerobic conditions, with a marked down-regulation of the *nir*, *nor* and *nos* genes under microaerobic conditions. The *Brucella* spp. NtrY protein contains one haem group for sensing the oxygen status in the cell and shows its maximal activity as an autohistidine kinase in the ferrous state under low oxygen tension [30,31].

Analysis of the whole genome sequence of *P. denitrificans* reveals the presence of genes encoding NtrBC and NtrYX proteins. In this work, we explore the global transcriptomic changes that underpin the transition from ammonium-dependent to nitrate-dependent aerobic growth, including the relationships within the different two-component regulatory systems NasTS, NtrBC and NtrYX. An additional mechanism to the transcriptional regulation of nitrate assimilation, based on a nitrate-dependent translation control of the *P. denitrificans* PD1222 Nas proteins, is also proposed.

MATERIALS AND METHODS

Bacterial strains, media and growth conditions

All strains used in this study are listed in Table S1. *P. denitrificans* PD1222 was grown at 30 ^{o}C in Luria-Bertani (LB) medium [32] or defined mineral salts medium as previously described [33], containing 50 mM succinate as carbon source. Ammonium chloride, potassium nitrate, potassium nitrite or L-glutamate were used as nitrogen source (10 mM each), as stated in the text. Bacteria were cultured in 250 mL flasks containing 50 mL of medium that were rotated at 200 rpm. *E. coli* strains were grown at 37 ^{o}C in LB medium. Cell growth was followed measuring the absorbance of the cultures at 600 nm (A_{600}) or by protein determination [34]. Antibiotic supplements were used at the following concentrations ($\mu g \cdot mL^{-1}$): ampicillin (Amp), 100; kanamycin (Km), 25; rifampicin (Rif), 100; spectinomycin (Sp), 25; streptomycin (Sm), 60; tetracycline (Tet), 10; chloramphenicol (Cm), 50.

Analytical methods

Upon reaching exponential growth phase, a 50 mL culture volume was subject to cell fractionation. Cells were harvested, washed twice with 50 mM Tris-HCl (pH 8.0) and re-suspended in 10 mM Tris-HCl (pH 8.0), 500 mM sucrose and 3 mM EDTA. Lysozyme (chicken egg white, EC 3.2.1.17) at 0.2 $mg \cdot mL^{-1}$ final concentration and a few grains of DNase I (bovine pancreas, EC 3.1.21.1) were added. This mixture was incubated with shaking for 30 minutes at 30 ^{o}C. The sphaeroplasts formed were harvested by centrifugation (13000 x g) for 15 minutes at 4 ^{o}C and the periplasm was recovered. Sphaeroplasts were re-suspended in a volume of 10 mL 100 mM Tris-HCl (pH 8.0) and disrupted by sonication, and cytoplasmic and membrane fractions were separated by ultracentrifugation (40000 x g). Assimilatory NADH-dependent nitrate reductase activity was assayed in cytoplasmic fractions in the presence of NADH as electron donor by measuring the nitrite formed from nitrate [35]. β-galactosidase activity was determined spectrophotometrically as previously described [36]. Protein concentration was measured by using a Bradford protein assay kit (Bio-Rad, UK) with a BSA standard (Fraction V, Sigma, UK).

Microarray analysis of *P. denitrificans*

P. denitrificans genomic DNA was isolated using a Genomic DNA extracting kit and 100/G columns (Qiagen) from 10 mL exponential phase cells according with the specification of the manufacturer. For RNA extractions, 30 mL of early-exponential phase cells (A_{600} ~ 0.4) was added to 12 mL of ice-cold 95% ethanol/5% phenol (v/v) solution, and incubated on ice for 30 minutes to prevent RNA degradation. Cells were then pelleted and stored at -80 °C until RNA was extracted by using SV Total RNA isolation kit (Promega). Trace DNA contamination was removed by treatment with Turbo DNA-*free*™ DNase (Ambion), and this was confirmed by PCR amplification of RNA samples using MyFi™ DNA polymerase (Bioline). Nucleic acids were quantified spectrophotometrically in a Nanodrop 2000 (Thermo Scientific), and integrity of RNA samples was analyzed using an Experion™ Automated Electrophoresis platform (BioRad) using RNA StdSens chips (BioRad). All standard protocols were carried out according with the instructions of the manufacturers.

For labelling and hybridisation of microarray slides, total RNA (10 μg) from three independent bacterial cultures were reverse-transcribed to cDNA using

AffinityScript multiple temperature reverse transcriptase (Agilent), and fluorescently labelled using random primers (Invitrogen) to incorporate Cy5-dCTP (Amersham). *P. denitrificans g*enomic DNA (10 µg) was labelled with Cy3-dCTP (Amersham) using a Bioprime® DNA labelling system (Invitrogen), prior to mixing (1:5) with labelled cDNA and hybridised to custom-designed 4 x 44K oligonucleotide array slides (Agilent). Hybridisation buffer (50 mM morpholine-4-ethanesulfonic acid pH 6.5, 1 M NaCl, 20% w/v formamide, 20 mM EDTA, 1% w/v, Triton-X-100) mixed with Cy5- and Cy3-dCTP labelled nucleic acids were loaded onto the GASKET slide prior to placing the microarray slide in contact with the hybridization mix, which were sealed in a tight chamber and incubated at 55 °C in a rotary hybridisation oven at 8 rpm, for approximately 60 hours in the dark. Following hybridizations, slides were removed and washed for 5 minutes in a microscope-slide chamber using a solution of 6 x SSPE (0.2 M phosphate buffer, 2.98 M NaCl, 20 mM EDTA, pH 7.4) supplemented with 0.005% N-lauryl-sarcosine, followed by 5 minutes in a solution of 0.6 x SSPE supplemented with 0.18% polyethylene glycol 200. Slides were then dried by centrifugation for 30 seconds.

For analyses and interpretation, microarray slides were scanned using a scanner (GenePix 4000A, Axon Instruments) with excitation wavelengths of 532 nm and 635 nm. Fluorescent spots and background intensities were quantified using GenePix Pro software (Axon Instruments) and filtered to omit those with a reference signal lower than two standard-deviations from the background intensity in further analyses. Signal intensities were corrected by subtracting the background and the red/green (Cy5/Cy3) ratios. All datasets were normalised using Batch Anti-Banana Algorithm in R (BABAR) which uses cyclic loess to normalise across the complete dataset [37] and analyzed using Gene Spring 7.3 (Agilent) to filter genes that were differentially expressed ≥ 2-fold with significance of ≥ 95% across three independent cultures. These data are represented in Figure 1, where $\log_2$ of normalised expression values are shown as a heat-map. Microarrays were validated by qPCR with oligonucleotide primers that annealed to internal regions of the *nas* genes (Table S2), as described below. Primers were designed using Primer^3 Plus software [38], to amplify products between 100 and 150 bp, with a T_m of about 60 °C and used at a final concentration of 0.4 µM. The relative fold-change values were calculated by using amplification efficiencies, as described previously [39].

Proteomic analysis

Two-dimensional gels electrophoresis (2D-PAGE) was performed with sample preparations that were obtained from *P. denitrificans* cells grown to mid-log phase in minimal medium with different nitrogen sources as previously described [2]. Subcellular fractionation was carried as described above, and isolated cytoplasmic fractions containing 250 µg protein were used to rehydrate 11 cm strips (Immobiline DryStrips with the appropriate pH range; Amersham Biosciences) for 12 h. Isoelectric focusing was carried out in an IPGphor (Pharmacia) until 20000 volt-hours were reached. After isoelectric focusing, strips were equilibrated as previously described [40] and applied to 12% (v/v) polyacrylamide gels. Second dimension SDS-PAGE was performed by using the Hoefer SE600 system (Amersham Biosciences) and gels were stained using the Brilliant Blue G-colloidal concentrate (Sigma) and scanned with a Molecular Image FX (Bio-Rad). Triplicate 2D-PAGE separations were generated for each sample. Protein identification was carried out in the UCO-SCAI Proteomic Centre,

University of Córdoba (Spain), a member of ProteoRed network. Protein spots of interest were excised automatically in a ProPic station (Genomic Solutions, UK) and samples were automatically digested with trypsin according with standard protocols in a ProGest station (Genomic Solutions), and analyzed in a 4700 Proteomics Analyzer MALDI-TOF/TOF mass spectrometer (Applied Biosystems), in the m/z range 800 to 4000, with an accelerating voltage of 20 kV, in reflectron mode and with delayed extraction set to "on" and an elapsed time of 120 ns. Proteins were identified by peptide mass fingerprinting (PMF) and confirmed by MS/MS analysis of the three most abundant peptide ions. MASCOT searching engine (Matrixscience, UK) was used for protein identification over the non-redundant NCBI database of proteins. The confidence in the peptide mass fingerprinting matches ($p < 0.05$) was based on the MOWSE score (higher than 65) and CI > 99.8%, and confirmed by the accurate overlapping of the matched peptides with the major peaks of the mass spectrum.

Routine DNA manipulations and site-directed mutagenesis of *nasA* leader sequence

Genomic and plasmid DNA were routinely isolated and purified using the Wizard® Genomic DNA purification kit (Promega, USA) and the Qiagen plasmid kit (Qiagen, Germany), respectively. Custom oligonucleotide primers, listed in Table S2, were supplied by Invitrogen (Paisley, UK) and the polymerase chain reaction (PCR) was performed using the Expand High Fidelity PCR system (Roche, Switzerland) with 5% DMSO added as standard.

In the mutational analysis carried out *in trans* of the *nasA* leader region, a *nasA* promoter transcriptional fusion was constructed by using an intergenic *nasS-nasA* 392-bp fragment amplified by PCR with oligonucleotides FA1_A/RA1, which were located at the 3´-end of *nasS* and at the 5´-end of *nasA*, respectively. This fragment was cloned within the pSparkII vector and subcloned as *Sph*I-*Pst*I in the promoter probe vector pMP220, generating pMP220-*P*nasA (Table S1). Different mutated versions of *P*nasA-*lacZ* were also constructed by using oligonucleotides containing substitutions of three bases for two hairpins, HI or HII, identified in the *nasA* gene leader region (HI 137 bp and HII 91 bp upstream 5´-end *nasA* gene, respectively). Oligonucleotides FA1_B/RHI and FHII/RA1 were used for mutagenesis of hairpins I or II, respectively, and the PCR products amplified with these oligonucleotides were cloned into the pSparkII vector. The pMP220-*P*nasA vector was digested with *Pst*I/*Asc*I and used to clone the mutated fragment of the hairpin I previously liberated from pSparkII with *Pst*I/*Asc*I restriction enzymes, obtaining the pMP220-*P*nasA1 construct. The pMP220 plasmid is a non-integrative vector. For mutagenesis of hairpin II, the corresponding mutated fragment was liberated from pSparkII with *Asc*I/*Sph*I and cloned into pMP220-*P*nasA previously digested with *Asc*I/*Sph*I, obtaining pMP220-*P*nasA2 plasmid. All constructs were sequenced (UCO-SCAI, University of Córdoba) to confirm the native or the mutated sequences and the final constructs were introduced into *P. denitrificans* PD1222 by triparental mating [2].

In the mutational analysis carried out *in cis* of the ANTAR region (hairpin I), the DNA regions upstream and downstream this secondary structure were amplified by PCR with oligonucleotide pairs AIF1/AIR1a and AIF2/AIR2, respectively. These two fragments were cloned separately into the pSparkII cloning vector. The upstream fragment (524 bp) was subcloned as *Eco*RI/*Sal*I into pK18mobsacB, a kanamycin-resistant suicide vector in *Paracoccus denitrificans*. The downstream fragment (578 bp) was subcloned as *Sal*I/*Hin*dIII into the previous construction. The final construction

contained a 35 bp sequence corresponding to the multicloning site of the pSparkII vector replacing the native hairpin I sequence (37 bp). This plasmid was used for triparental mating with the receptor strain *Paracoccus denitrificans* and the helper strain *E. coli* containing the pRK2013 plasmid. First transconjugant selection was carried out in LB media with spectinomycin and kanamycin. After that, a sucrose selection for double-crossover events was performed. Finally, mutation was confirmed by PCR and enzyme restriction analyses. The wild-type *nasA* leader region with hairpin I was amplified with oligonucleotides FA1_A/RA1. This wild-type fragment was not digested by *Sal*I, whereas the fragment amplified from the mutant was digested by this restriction enzyme because it contains the *Sal*I recognition sequence of the pSparkI multicloning site.

Site-directed mutagenesis of the NtrC binding sequence

The native *nasT* promoter, as well as a mutated version affected in the putative NtrC binding site located upstream of *nasT* gene, were used to generate transcriptional fusions by PCR-driven overlap extension. Initial PCRs were carried out with oligonucleotides PTF/PTNtrR and PTR/PTNtrF for the native construct, and PTF/PTNtrR_Mut and PTR/PTNtrF_Mut for the mutated version. Internal primers (PTNtr) were used to generate overlapping and complementary 3´-ends on the intermediate segments. In the case of the mutated *nasT* promoter, the PTNtr primers were also used to introduce the mutated bases. Overlapping strands hybridize at this region in a subsequent PCR and were extended to generate the full-length product (619-bp) amplified by flanking primers that include restriction enzyme sites for cloning as *Pst*I/*Sph*I into the promoter probe vector pMP220. The final constructs for the analysis of the native *nasT* promoter and the NtrC-binding site mutated version of *nasT* promoter were called pMP220-*P*nasT and pMP220-*P*nasT1, respectively. All plasmids were checked by sequencing (UCO-SCAI, University of Córdoba) and the final constructs were introduced into *P. denitrificans* PD1222 by triparental mating [2].

RT-PCR and qPCR reactions

P. denitrificans wild-type and mutant strains were cultured in minimal medium with succinate as carbon source and different nitrogen sources. Cells were harvested (A_{600} ~ 0.4) and washed in TEG buffer with 25 mM Tris-HCl (pH 8.0), 1% glucose and 10 mM EDTA. RNA isolations were performed following the Qiagen RNA extraction kit (RNeasy midi kit). DNase incubation was carried out in the column with RNase-free DNase set (Qiagen) and an additional post-column treatment was required with DNase I (Ambion). The concentration and purity of the RNA samples were measured in a ND1000 spectrophotometer (Nanodrop Technologies). Synthesis of total cDNA was achieved in 20 µL final volume, containing: 500 ng RNA, 0.7 mM dNTPs, 200 U SuperScript II Reverse Transcriptase (Invitrogen) and 3.75 µM random hexamers (Applied Biosystems). Samples were initially heated at 65 ºC for 5 min and then incubated at 42 ºC for 50 min, followed by incubation at 70 ºC for 15 min. To carry out PCR reactions, 2 µL of each cDNA were initially heated at 98 ºC for 2 min, followed by 30 cycles of amplification: 98 ºC, 30 s; 60 ºC, 30 s and 69 ºC, 1 min. Polymerase extension reactions were completed by an additional incubation at 69 ºC for 10 min**.** For real-time assays, the cDNA was purified using Favorprep Gel/PCR purification kit (Favorgen) and the concentration was measured using a ND1000 spectrophotometer. The iQ5 Multicolor Real-Time PCR Detection System (Bio-Rad) was used in a 25 µL reaction (final volume), containing 2 µL diluted cDNA (12.5, 2.5 and 0.5 ng), 0.2 µM of

each primer (Table S2), and 12.5 µL iQ SYBR Green Supermix (Bio-Rad). Target cDNAs and reference samples were amplified three times in separate PCR reactions. Samples were initially denatured by heating at 95 ºC for 3 min, followed by 40 cycles of amplification (95 ºC, 30 s; test annealing temperature, 60 ºC, 30 s; elongation and signal acquisition, 72 ºC, 30 s). For relative quantification of the fluorescence values, a calibration curve was made using dilution series from 100-0.001 ng of *P. denitrificans* genomic DNA sample. Represented data were normalized by using the *rpoB* and the *dnaN* genes as housekeeping (Table S2). Primer design and relative fold-change values calculation were carried out as previously described [38,39].

Generation of *ntrB* and *ntrY* mutant strains of *P. denitrificans*

Mutant strains of *P. denitrificans* were generated by significant allelic replacement with specific antibiotic resistance markers. The *ntrB* mutant (*ntrB*Δ::Sm) was generated by PCR amplification of the 3´-end (682 bp) and 5´-end (533 bp) of the *ntrB* gene with the respective set of primers ntrB1/ntrB2 and ntrB3/ntrB4 (Table S2). The PCR products were cloned within the pGEM-T Easy vector and then assembled within pUC18 vector (Table S1). A unique *Bam*HI restriction site was generated at the interface of the 3´-end and the 5´-end of *ntrB* gene to generate a 685 bp deletion and to insert a streptomycin resistance cassette from the pSRA2 vector (Table S1). A single *Eco*RI fragment (*ntrB*Δ::Sm) was transferred to pSUP202 to produce the final mobilizable vector.

For the *ntrY* mutant strain (*ntrY*Δ::Km), fragments containing the 3´-end (510 bp) and 5´-end (717 bp) of *ntrY* were produced by PCR using the respective primer pairs ntrY1/ntrY2 and ntrY3/ntrY4 (Table S2) and cloned within the pGEM-T vector (Table S1). The upstream region was screened by restriction digestion and selected by using an *Eco*RI recognition site and the downstream region of *ntrY* was introduced as an *Aat*II-*Bam*HI fragment, yielding a unique *Bam*HI restriction site between both regions, generating a 1035 bp deletion. A kanamycin resistance cassette obtained from the pSRA2 vector (Table S1) was inserted as a *Bam*HI fragment between these regions of *ntrY*. Finally, the *Aat*II-*Eco*RI fragment (*ntrY*Δ::Km) was cloned into the mobilizable vector pSUP202. This construct was transferred to either the wild-type strain or the *ntrB* mutant to generate the single *ntrY* or the double NtrB/NtrY mutant, respectively. Plasmids were analyzed by DNA-sequencing (UCO-SCAI, University of Córdoba) and mutants were checked by PCR by using primer pairs that amplify for a product containing the deletion-insertion mutation. Mutants showed bands higher than those presented in the wild type because the inserted resistance cassettes were larger than the deleted fragments, confirming allelic exchange by double-crossover mechanism.

RESULTS

Transcriptomic differences between bacteria cultured aerobically under nitrate- versus ammonium-dependent anabolism

To investigate the underlying biochemical adaptation to nitrate assimilation compared to ammonium-dependent anabolism, transcriptomic analysis was undertaken through microarray analysis of RNA isolated from *P. denitrificans* cells grown in batch culture with 20 mM succinate and either 10 mM nitrate or 10 mM ammonium as the sole N-source. Of the 5077 protein-coding genes that are present in the genome of *P. denitrificans* PD1222, only 83 genes (1.64 % of the whole genome) displayed at least 2-fold expression differences at a 95% significance level between the two growth conditions tested. Among these, 74 genes were induced during nitrate-dependent growth, while 9 genes were down-regulated (Fig. 1A).

The genes induced when nitrate was the only nitrogen source belonged to 30 gene clusters, including among others, the *gltB* and *gltD* genes encoding the small and large subunits of the glutamate synthase (GOGAT), the *amtB* gene that codes for a high-affinity ammonium transporter, the *ntrB* and *ntrC* genes that code for the general nitrogen regulatory Ntr system, the *glnB* gene that codes for the nitrogen regulatory protein PII, the *glnA* gene encoding the glutamine synthetase (GS), the *bztA-D* gene cluster involved in glutamate/aspartate transport, the *ureA-GJ* gene cluster for urea metabolism, the *urtA-E* gene cluster for urea transport, the *potDF-I* gene cluster involved in polyamine transport, the *braC-G* gene cluster involved in branched-chain amino acids transport, the *dctPQM* genes encoding a TRAP dicarboxylate transporter system, the respiratory nitrate reductase *narGJ* genes, and the *nasTSABGHC* gene cluster for nitrate/nitrite assimilation (Fig. 1A). The genes down-regulated during growth with nitrate included the *gdhA* gene that encodes the glutamate dehydrogenase (Fig. 1A). Expression of a selection of these genes was also quantified by qPCR and corroborated well with the microarray data (Table 1). The genes for which expression was highly increased on nitrate included *nasA, nasH, narG, narJ, nasT*, *nasS, urtC*, *amtB, ureD, glnA*, *glnB, gltD,* and *ntrC.* The *nasT* gene was more strongly induced by nitrate than the *nasS* gene (Table 1).

Qualitative proteomic analysis by 2D-PAGE of soluble fractions of *P. denitrificans* cells grown with nitrate or ammonium as the sole N-source confirmed that a significative number of the key changes in the transcriptome could be also indentifed in the proteome (Fig. 1B). The up-regulated proteins for which higher levels of synthesis in the presence of nitrate could be confirmed included the nitrogen regulatory protein GlnB (PII), the periplasmic component of the urea ABC-type transporter (UrtA), the polyamine transporter component (PotD), the glutamate/aspartate transporter component (BztA), and two proteins encoded by the *nas* gene cluster of *P. denitrificans* (NasG and NasB). A decreased synthesis of the glutamate dehydrogenase (GdhA) was observed in the nitrate grown cells compared to the ammonium-grown cells (Fig. 1B).

Analysis of the expression of the *nasTS and nasABGHC* transcripts

The transcriptome differences between nitrate- and ammonium-anabolising cells suggest a general adaptation to metabolism of secondary (non-ammonium) nitrogen sources, nitrogen scavenging and the need to search for organic carbon to provide the reductant for nitrate assimilation. Alongside this is a more specific adaptation to nitrate anabolism through expression of the *nasABGHC* genes. Therefore, the control of the

nas gene expression was investigated. The regulatory pattern for *P. denitrificans nas* gene expression was analyzed at the transcriptional level by RT-PCR analysis with RNA from cells grown with nitrate, glutamate, ammonium, or ammonium plus nitrate as N-source. Primer pairs were designed to explore transcription across the 3'- and the 5'-ends of different *nas* gene boundaries (Fig. 2A). The PCR products were detected across the *nasTS, nasAB, nasBG, nasGH, nasHC*, and *nasGHC* boundaries (Fig. 2B). However, PCR product was undetectable when the primers located at the 3'-end of the *nasS* gene and the 5'-end of the *nasA* gene were used. These results suggest that the *nasTSABGHC* gene cluster comprises two different transcriptional units, one corresponding to the regulatory *nasTS* genes and the other constituted by the structural *nasABGHC* genes.

The RT-PCR analysis also indicated that the *nasA-C* transcript is found in cells grown with either nitrate or glutamate as sole N-source, but not when ammonium was present (Fig. 2). However, a high glutamine concentration (5 mM) or a 2-oxoglutarate/glutamine 5 mM/5 mM ratio did not repress expression of the *nas* genes. The *nasA* gene expression, determined by RT-qPCR, was similar in cells grown with glutamate or glutamate plus nitrate (Fig. 2C). The *nasTS* transcript was detected in cells grown with all nitrogen sources tested, although only at very low levels in the presence of ammonium (Fig. 2C).

A proteomic approach was applied to confirm the presence of polypeptides encoded by the *nas* genes in cytoplasmic fractions of *P. denitrificans* cells grown with different nitrogen sources. The Rieske-type protein NasG required for both nitrate and nitrite reductase activities (Fig. 3A) and the catalytic subunit of the nitrite reductase NasB (not shown) were only detected when nitrate was present in the media and ammonium was absent. NADH-dependent nitrate reductase activity was determined in the cytoplasmic fraction from cells grown with different nitrogen sources. In accordance with the proteomic analysis, the nitrate reductase activity was detected only in presence of nitrate and absence of ammonium (Fig. 3A). It is notable that although the *nasABGHC* transcript was detected in cells grown with glutamate in absence of nitrate (Fig. 2B), the NasG and NasB proteins and the nitrate reductase activity were not detectable under these conditions (Fig. 3A).

Analysis of *nas* gene expression in the *nasT* and *nasS* mutants

It has been previously described that a *nasT* mutant of *P. denitrificans* is unable to grow with nitrate as the sole nitrogen source, whereas a *P. denitrificans nasS* mutant grows with nitrate as the sole N-source with similar rate and yield to the wild-type strain [5]. To analyze the regulatory effect of nitrate in the *nasS* and *nasT* mutants, a comparison of *nas* gene expression between cells grown with glutamate versus cells grown with glutamate plus nitrate was performed. RT-qPCR analysis showed that the *nasT* mutant lacks the *nasABGHC* transcript (Fig. 3B). Accordingly, 2D-PAGE revealed that this mutant strain is also devoid of the NasG polypeptide (Fig. 3C). It is noticeable that the respiratory nitrate reductase *narG* and *narJ* genes were up-regulated in the *nasT* mutant strain, whereas genes coding for glutamine synthetase (*glnA*) and PII regulatory protein (*glnB*) were down-regulated (Table 2), suggesting that NasT might also serve as part of a more complex global regulatory system.

In the *P. denitrificans nasS* mutant, the *nasABGHC* transcript was detected in all nitrogen sources, except when ammonium was used as N-source, similarly to the wild-type strain (Fig. 3B). The NasG polypeptide and the nitrate reductase activity were

detected in the *nasS* mutant strain grown with glutamate both in presence and absence of nitrate (Fig. 3C), whereas in the wild-type strain the NasG polypeptide and the nitrate reductase activity were detected only in the presence of nitrate (Fig. 3A). In addition, RT-qPCR analysis revealed that the *nasS* mutant strain showed significantly increased levels of the *narG* and *gdhA* genes in response to nitrate (Table 2).

Identification of putative *cis*-regulatory RNA secondary structures in the *nasA* leader region

Between the regulatory *nasTS* genes and the structural *nasABGHC* genes lies a ~200 bp non-coding region with putative hairpin structures that could lead to transcription termination (Fig. 4A). Secondary structures in the RNA leader sequence of *nasA* are thought to terminate transcription [14,15], but binding of NasT could allow transcription antitermination. Putative hairpin structures that could be a target for the transcriptional antiterminator NasT in the *nasA* leader region were identified by using the RNAfold web server http://rna.tbi.univie.ac.at/cgi-bin/RNAfold.cgi. To explore the importance of this region, several *lacZ* transcriptional fusions were constructed and expressed in *P. denitrificans* cells grown with either nitrate or ammonium as sole N-source. In cells grown under nitrate anabolizing conditions, the mutation of the HI hairpin resulted in a severe deficiency in the transcriptional activity. However, transcriptional activity was relatively unaffected in the HII mutation (Fig. 4B). In cells grown with ammonium the transcriptional activity was 100-fold lower than in nitrate-assimilating cells, but there was a two-fold increase in cells carrying the HII mutation. These results suggest that the HI hairpin is important for NasT binding, and that HII structure may contribute to transcription attenuation. To corroborate the importance of HI, a specific chromosomal mutation *in cis* of the putative NasT binding region was introduced. This chromosomal mutant lost the parental capacity to grow with nitrate as the sole nitrogen source (Fig. 4C). Controls established that the chromosomal HI mutant strain showed a similar growth to the parental strain with ammonium as nitrogen source.

The contribution of *ntrBCYX* to the regulation of nitrate assimilation

In addition to *nasTS* genes, the *ntrBC* genes were also up-regulated during nitrate-dependent anabolism compared to cells grown with ammonium (Fig. 1A, Table 1). This suggests an integrated regulation of nitrate metabolism between these two systems. The *ntrBC* genes are clustered together with the *ntrYX* genes. The *ntrB* gene encodes a signal transduction protein (386 residues) with histidine kinase activity involved in nitrogen metabolism, and the *ntrC* gene codes for a Fis-like σ^{54}-dependent regulator receiver protein (486 residues). Similarly, the *ntrY* gene codes for a multi-sensor signal transduction regulator (709 residues) with histidine kinase activity and the *ntrX* gene encodes a σ^{54}-dependent regulatory protein (463 residues). A non-coding region of 217 bp lies between *ntrC* and *ntrY* genes, whereas *ntrY* and *ntrX* genes overlap by 3 bp. NtrB and NtrC homologues have been found in many different microorganisms (Fig. S1). Although the NtrYX system is not widely distributed among bacteria, the *P. denitrificans* NtrY protein showed the highest identity (41%) with *Azorhizobium caulinodans* NtrY, whereas the *P. denitrificans* NtrX protein showed the highest identity (56%) with its homologues in *Azorhizobium caulinodans* and *Azospirillum brasilense* (Fig. S2).

Isolation and characterization of single *ntrB* and *ntrY* mutants and double *ntrB*/*ntrY* mutant of *P. denitrificans* were carried out. All mutant strains displayed similar growth rates and yields to that shown by the wild-type strain when ammonium

was used as nitrogen source. However, the *ntrY* mutant was only slightly affected on its growth on nitrate, whereas the *ntrB* mutant showed a longer lag-phase than the wild-type, and the double *ntrB*/*ntrY* mutant was unable to grow with nitrate (Fig. 5A).

Expression of the *nasT*, *nasS*, *ntrB*, *ntrY* regulatory genes and the structural *nasA* gene was analyzed by RT-qPCR in the *ntrB* and *ntrY* mutants and the wild-type strain of *P. denitrificans*. In the *ntrB* mutant *nasTS* and *nasA* were down-regulated (Fig. 5B), whereas in the *ntrY* mutant all these genes were expressed similarly to the wild-type strain (not shown). The assimilatory NADH-dependent nitrate reductase activity was determined in cytoplasmic fractions from wild-type, *ntrB* and *ntrY* mutants grown with nitrate, when all strains reached similar biomass (protein concentration about 150 mg mL^{-1}). The *ntrY* mutant showed similar levels of activity to that presented by the wild-type, about 4 nmol NO_2^- formed min^{-1} mg^{-1}, whereas the *ntrB* mutant only presented an activity of about 1 nmol NO_2^- formed min^{-1} mg^{-1}.

Transcriptional fusions to the β-galactosidase-encoding gene *lacZ* were carried out in the *nasT* leader sequence and expressed in the wild-type, *ntrB* and *ntrY* mutant strains of *P. denitrificans*. The β-galactosidase activities in the *ntrY* mutant were very similar to those found in the wild-type strain (Table 3). However, β-galactosidase activities in the *P. denitrificans ntrB* mutant were much lower than those described for the wild-type strain (Table 3).

These data strongly suggest a role for NtrBC in the regulation of nitrate assimilation at the level of expression of *nasT* and so the possibility of a *cis*-acting binding site for NtrC was explored. The RegPrecise program for collection of manually curated inferences of regions in prokaryotic genomes identified a very well conserved putative NtrC binding site (5′- (T/C)GC(C/A)NNNNTTNNT(G/A)GCA-3′) in the leader regions of a number of the different genes in *P. denitrificans,* including the *glnBA*, *amtB,* and *nasTS* genes. These genes were upregulated during nitrate assimilation, as revealed by the transcriptomic analyses (Fig. 1A, Table 1). Several base pairs were mutated in the putative NtrC binding site located in the *nasT* leader sequence, resulting in the loss of the up-regulation observed under nitrate- or glutamate-dependent growth conditions (Table 3). These results highlight the importance of this sequence motif in the regulation of nitrate assimilation.

DISCUSSION

The soil denitrifier *P. denitrificans* can use nitrate as the sole N-source by an assimilatory nitrate reduction system. The process of nitrate assimilation in this bacterium has been comprehensively investigated by comparative transcriptomic and proteomic analyses in cells grown under nitrate- or ammonium-assimilating conditions (Figs. 1, 3 and S3). Comparing nitrate- to ammonium-grown cells, a key metabolic change was the decrease in the expression of glutamate dehydrogenase, the enzyme related with the low affinity ammonium assimilation pathway. This was accompanied by induction of components for organic nitrogen scavenging, urea uptake and utilisation, high affinity ammonium uptake and assimilation, regulatory and structural components of inorganic nitrate and nitrite assimilation, and scavenging of dicarboxylate organic acids to provide the additional reducing equivalents required for nitrate assimilation (eight electrons per nitrate ion converted into ammonia).

In *P. denitrificans,* the regulatory *nasTS* genes are located at the 5′-end of the *P. denitrificans nas* gene cluster for nitrate assimilation (Fig. 2A). RT-PCR and qPCR analyses of the *P. denitrificans nasTS* and *nasABGHC* genes demonstrate that these genes are transcribed as separated transcriptional units. The existence of two independent transcriptional units in the *P. denitrificans nas* region is also supported by the presence of a non-coding region between the regulatory *nasTS* genes and the structural *nasABGHC* genes, with two putative hairpins (HI and HII) that could lead to secondary structures in this mRNA region (Fig. 4). These two transcriptional units show different regulation, since expression of the regulatory *nasT* and *nasS* genes was observed in all N-sources tested, including ammonium, although in general at very low levels, whereas *nasABGHC* transcript was detected either with nitrate or glutamate, but it was undetectable with ammonium independently of the presence or absence of nitrate (Fig. 2). However, although the *nasABGHC* transcript was present in wild-type cells grown with glutamate as the sole N-source, the Rieske-type NasG protein and the large subunit of the assimilatory nitrite reductase NasB, required for both nitrate and nitrite reductase activities, were not detected by 2D-PAGE and these proteins were only observed in the presence of nitrate. Accordingly, the assimilatory NADH-dependent nitrate reductase activity was not detected when glutamate was used as the sole nitrogen source (Fig. 3A). These results suggest that nitrate is not an obligate inducer of the *nasABGHC* gene expression, and that it may also play a positive role at the translational level.

Mutational analysis of the *nasT* gene of *P. denitrificans* reveals that NasT could act as transcription antiterminator because the *nasT* mutant strain is unable to grow with nitrate as the sole N-source and lacks both *nasABGHC* transcript and NADH-nitrate reductase activity (Fig. 3BC). Also, the strain harbouring the chromosomal mutation in a putative *cis*-acting NasT binding site (hairpin I) was unable to grow with nitrate (Fig. 4C). Therefore, in this work we have identified the RNA region where NasT is likely to bind as a transcriptional antiterminator. On the contrary, the *nasS* mutant strain of *P. denitrificans* is capable to use nitrate as the sole N-source, similarly to the wild-type strain, but shows a deregulated nitrate reductase activity that can be detected independently of the presence or absence of nitrate (Fig. 3BC). In addition, assimilatory nitrate reductase activity in the *P. denitrificans nasS* mutant is abolished in the presence of ammonium, as previously described in the wild-type strain [5]. Expression of the *nasT* gene is higher than *nasS* gene expression (Tables 1 and 2), probably because

strong secondary structures present at the 5′-end of the *nasS* gene might provoke RNA polymerase to be occasionally released without completing the whole transcript.

P. denitrificans NasS and NasT proteins expressed in *E. coli* have been purified as a tetrameric complex in the absence of nitrate or nitrite, but in addition to the NasT-NasS complex, free NasT protein can be also detected [5]. Therefore, in the absence of nitrate, NasS and NasT form a protein-protein complex, probably with two units of each protein, which limits binding of NasT to the *nas* mRNA to act as transcription antiterminator. However, in the presence of nitrate, NasS clamps the oxyanion, changing conformation and dissociates from NasT, thus increasing the size of the free NasT pool available to serve for *nasABGHC* transcription antitermination [5]. However, the elevated *nasT* gene expression over the *nasS* gene could lead to an excess of NasT protein over the NasS protein. This unbalance implies that there is always enough free NasT to allow transcription of *nasABGHC* genes in the absence of both nitrate and ammonium (i.e., glutamate as N-source), suggesting additional global regulatory roles. In the *P. denitrificans nasT* mutant the structural *nasABGHC* transcript was absent in all N-sources tested (Fig. 3B). This is consistent with a role for NasT as transcription antiterminator and with the phenotype of the *P. denitrificans nasT* mutant, which is unable to grow with nitrate or nitrite as the sole N-source. In addition, up-regulation of *narG* and *narJ* genes and down-regulation of *glnAB* genes in the *nasT* mutant also indicated that NasT may be involved in other regulatory processes. Recently, it has been suggested in the soybean endosymbiont *Bradyrhizobium japonicum* that *nasST* genes regulate respiratory nitrous oxide and periplasmic nitrate reductases [41]. Therefore, additional targets for NasT may exist in *P. denitrificans*, which could function as negative regulators of *nar* gene expression.

In the *nasS* mutant the *nasABGHC* gene expression is no longer under nitrate control because in the absence of the NasS protein, all the NasT pool is free to serve as transcription antiterminator under all growth conditions (Fig. 3BC). Thus, in contrast to the wild-type strain, the *nasS* mutant of *P. denitrificans* displayed in 2D-PAGE gels the assimilatory nitrite reductase NasB and the Rieske-type NasG polypeptides when glutamate was used as nitrogen source, independently of the presence or absence of nitrate (Fig. 3C). These results corroborate that nitrate exerts a regulatory control at post-transcriptional (translational) level in addition to the role of NasTS in the transcription antitermination.

The phenotypes of the *ntrB*, *ntrY* and *ntrB*/*ntrY* mutants of *P. denitrificans* suggest that the NtrBC system is mainly required for nitrate assimilation, while the NtrYX system only has a slight contribution (Fig. 5A). The regulatory *nasTS* genes and the structural *nasA* gene are down-regulated in the *ntrB* mutant of *P. denitrificans* (Fig. 5B), suggesting that these genes are under the control of the NtrBC system. This idea has been corroborated by using the *lacZ* gene transcriptionally fused to native and mutated *nasT* leader sequence (Table 3). These results indicate that, in the absence of ammonium, phosphorylated NtrC could bind to the *nasT* promoter region, where a consensus NtrC-binding site has been identified. The absence of the *nasABGHC* transcript in cells grown with ammonium also suggests that NtrC or NrtX may bind to an, as yet unidentified, site in the *nasA* leader region. According with the RegPrecise program, very well conserved putative NtrC binding sites are found in the promoter regions of the *nasT* and *ntrBC* genes, suggesting that these two gene clusters are under the regulation of the general nitrogen control.

The increased synthesis of *P. denitrificans nasABGHC* genes reflects a system-specific response to ammonium-limited growth in which nitrate is initially the sole available N-source [2]. This bacterium also uses nitrate as terminal electron acceptor by a membrane-bound nitrate reductase [1]. This respiratory nitrate reductase (Nar) can substitute for NasC (assimilatory nitrate reductase) during anaerobic growth. The present study shows that transcription of *nasTS* occurs at a low level in the presence of ammonium, whereas transcription of *nasABGHC* genes is fully repressed in cells grown with ammonium (Fig. 2). In *K. oxytoca*, *nasR* expression is sensitive to ammonium since it is induced by the NtrBC system when ammonium is absent [14]. In *Azotobacter vinelandii* expression of *nasST* genes is also sensitive to ammonium, although is not under the control of the Ntr system [17]. Nevertheless, the capacity for nitrate assimilation is lost in several *ntr* mutants [19]. Recently, it has been demonstrated that NtrBC and NasST co-regulate the *nasAB* genes required for nitrate/nitrite uptake and reduction in *A. vinelandii* [20]. Bioinformatic analysis has revealed that the two-component NasTS system is a regulatory mechanism for nitrate assimilation that is widely spread among bacteria. Particularly, NasT is mainly present in α-proteobacteria like Rhizobiales and Rhodobacterales, and β-proteobacteria like Burkholderiales [5]. NasTS is involved in the regulation of the assimilatory nitrate/nitrite reductase genes in response to nitrate or nitrite in *Azotobacter vinelandii, Pseudomonas putida* and *Rhodobacter capsulatus* [17,18,42]. However, in *Azotobacter vinelandii* these genes are arranged in the *nasST* orientation, instead of the *nasTS* organization found in *P. denitrificans,* and they do not cluster together with the *nas* genes encoding the nitrate/nitrite uptake and reduction system [43]. The NasS protein is homologous to proteins which belong to the ATP-dependent nitrate transport systems found in cyanobacteria, although NasS lacks the signal peptide for periplasmic translocation. This is consistent with the role of NasS as a nitrate/nitrite sensor rather than acting as the periplasmic component of the transport system for these oxyanions. The NasT protein is a regulator with the ANTAR binding domain characteristic of transcription antiterminators like the *Klebsiella oxytoca* NasR protein [4,14,16]. However, the *nasTS* genes are absent in the *nas* cluster of *Klebsiella*, in which they are functionally replaced by *nasR*, a gene mainly found in γ-proteobacteria. It has been proposed that NasR is both a nitrate/nitrite sensor and a transcription antiterminator. A hairpin structure in mRNA upstream from the *K. oxytoca nas* structural genes causes early termination of transcription [14]. It has been suggested that in the presence of nitrate or nitrite NasR binds to the mRNA transcript preventing hairpin formation. Additional novelty on the regulatory mechanisms for nitrate assimilation was found in *P. denitrificans* because repression of structural *nas* genes by ammonium could be directly exerted by ammonium itself rather than by glutamine or the glutamine/2-oxoglutarate ratio. Under low nitrogen conditions (absence of ammonium), the NtrB and NtrY proteins become active to phosphorylate their respective partners, NtrC or NtrX, which in turn, become active for binding to promoter regions of the regulated genes. In *R. capsulatus* the histidine kinases NtrB and NtrY can substitute for each other as phosphodonors towards the response regulator NtrC [29]. Also, a cross-talk between the NtrB/C and NrtY/X sensor/regulator pairs has been suggested in *A. brasilense* during nitrate-dependent growth [26]. However, NtrY protein is much larger than NtrB suggesting that they may play different functions. The NtrBC system is widespread among microorganism and displays known functions, like the control of genes for glutamine synthetase, amino acids transport, nitrate and nitrite assimilation, nitrogen fixation and, also for the expression of other nitrogen regulation genes. Although the role of the NtrBC system seems to be more related to nitrogen metabolism, in *A. brasilense* there is also a link

between this two-component regulatory system and polyhydroxybutyrate production [44]. To summarize, Fig. 6 represents the integration of mutational, transcriptomic and proteomic data to establish a novel regulation model of the nitrate/nitrite assimilation process in *P. denitrificans*, in which nitrate exerts a transcriptional and translational control that has no precedents in the literature as far as we know. In this model three conditions have been considered: i) presence of ammonium, in which the *nasABGHC* genes are repressed and there is a very low expression of the *nasTS* genes; ii) absence of both ammonium and nitrate (i.e. glutamate as N-source), in which *nasABGHC* and *nasTS* genes are expressed, but Nas polypeptides and nitrate reductase reductase activity are not detected; and iii) absence of ammonium and presence of nitrate, in which *nasABGHC* and *nasTS* genes are expressed and Nas proteins are synthesized, leading to an active nitrate assimilation system. Our experimental data supports the existence of a regulatory cascade with three levels of control. At level 1, the phosphorylated NtrC protein (and probably NtrX in a lesser extent) interacts with the *nas* promoter to activate *nas* gene expression in absence of ammonium, as described in other bacteria (general nitrogen control). Accordingly, a conserved NtrC-binding sequence has been found in the promoter region of the *nasT* gene. At level 2, the NasTS system controls expression of the *nasABGHC* genes by transcription antitermination. In the absence of nitrate, an inactive NasTS complex is formed but there is enough free NasT protein to allow transcription antitermination for the synthesis of a complete *nasABGHC* transcript, which is detectable in cells grown with glutamate. This NasT/NasS unbalance is probably a consequence of the high level of expression of the *nasT* gene compared to the *nasS* gene. At level 3, translation of the Nas proteins only occurs in the presence of nitrate. This regulation at the translational level may occur when NasS binds to nitrate and the NasTS complex dissociates, leading to an increase of free NasT protein that, in turn, may lead to up-regulation of systems involved in post-translational regulation.

This is a novel regulatory mechanism, but bioinformatics analyses may suggest that NasTS regulation is emerging in a wide number of bacteria, as previously reviewed [8]. As the *P. denitrificans* Nas system is very well characterized [2,5], this work may now lead to comparative studies in other bacteria, in which the NasTS system regulated nitrate assimilation and even other processes like nitrous oxide reduction, as recently described in *Bradyrhizobium japonicum* [41].

ACKNOWLEDGEMENTS

This work was supported by Ministerio de Ciencia y Tecnología (Grant BIO2015-64311-R) and Junta de Andalucía (Grant CVI-7560), Spain. DJR was a Royal Society and Wolfson Foundation for Merit Award Fellow and thank the Biotechnology and Biological Sciences Research Council (Grants BB/EO21999/1 and BB/D523019/1). This work was also funded by the Biotechnology and Biological Sciences Research Council (Grant BB/M00256X/1). VML-A was recipient of a postdoctoral fellowship from the Junta de Andalucía, Spain.

ABBREVIATIONS

ANTAR, Ami and NasR transcription antitermination regulator; Cy5-dCTP and Cy3-dCTP, deoxycytidine triphosphate containing either Cy5 or Cy3 dyes; dNTPs, deoxyribose-nucleoside triphosphates; EDTA, ethylenediaminetetraacetic acid; MALDI-TOF/TOF, matrix-assisted laser desorption/ionization (time of flight); NADH, nicotinamide adenine dinucleotide; NIT, N-terminal nitrate/nitrite sensor domain; Ntr, nitrogen regulator; RT-PCR, reverse transcription polymerase chain reaction; RT-qPCR, quantitative reverse transcription polymerase chain reaction; 2D-PAGE, two-dimensional polyacrylamide gel electrophoresis.

Table 1. Analysis by RT-qPCR of nitrate-induced genes detected in the microarrays of *P. denitrificans.*

Gene		NO_3^-/NH_4^+
Pden_0490	*gltD*	2.8 ± 0.5
Pden_0794	*bztB*	1.9 ± 0.4
Pden_1212	*ureD*	5.1 ± 1.8
Pden_2032	*amtB*	5.3 ± 1.7
Pden_2151	*potD*	2.6 ± 0.2
Pden_4019	*urtC*	6.2 ± 0.4
Pden_4129	*ntrC*	4.6 ± 0.5
Pden_4130	*ntrB*	1.6 ± 0.2
Pden_4234	*narJ*	24.3 ± 11.1
Pden_4236	*narG*	100.5 ± 23.3
Pden_4450	*nasH*	185.7 ± 9.8
Pden_4453	*nasA*	385.0 ± 11.9
Pden_4454	*nasS*	7.7 ± 1.5
Pden_4455	*nasT*	23.3 ± 6.3
Pden_4461	*glnB*	2.6 ± 0.6
Pden_4462	*glnA*	3.4 ± 0.7

Data correspond to the mean ± standard deviation of the nitrate/ammonium gene expression ratio.

Table 2. Analysis by RT-qPCR of nitrate-induced genes in the wild-type, *nasT* and *nasS* mutant strains of *P. denitrificans*.

Gene		Wild-type Glu+NO_3^-/Glu	*nasT* mutant Glu+NO_3^-/Glu	*nasS* mutant Glu+NO_3^-/Glu
Pden_0490	*gltD*	0.6 ± 0.1	0.7 ± 0.1	2.6 ±0.2
Pden_0794	*bztB*	2.2 ± 1.6	0.7 ± 0.4	-
Pden_1212	*ureD*	1.1 ± 0.4	1.0 ± 0.1	1.8 ± 0.1
Pden_2032	*amtB*	0.4 ± 0.0	0.6 ± 0.1	0.3 ± 0.1
Pden_2151	*potD*	0.5 ± 0.1	0.6 ± 0.1	-
Pden_4019	*urtC*	0.5 ± 0. 1	0.5 ± 0.1	-
Pden_4129	*ntrC*	0.4 ± 0.1	0.5 ± 0.1	0.8 ± 0.2
Pden_4130	*ntrB*	0.7 ± 0.1	0.6 ± 0.2	0.6 ± 0.1
Pden_4234	*narJ*	7.7 ±1.2	57.0 ± 14.4	-
Pden_4236	*narG*	2.5 ± 0.2	67.5 ± 12.2	173.8 ±12.3
Pden_4450	*nasH*	0.6 ± 0.2	0.9 ± 0.1	0.2 ± 0.1
Pden_4453	*nasA*	0.9 ± 0.3	0.3 ± 0.1	0.2 ± 0.1
Pden_4454	*nasS*	1.0 ± 0.3	1.4 ± 0.1	0.0 ± 0.0
Pden_4455	*nasT*	2.0 ± 0.4	0.0 ±0.0	1.8 ± 0.1
Pden_4461	*glnB*	2.0 ± 0.2	0.4 ± 0.1	1.0 ± 0.1
Pden_4462	*glnA*	1.7 ± 0.1	0.4 ± 0.1	1.2 ± 0.1
Pden_3872	*gdhA*	2.0 ± 0.3	1.1 ±0.2	11.4 ± 1.0

Data correspond to the mean ± standard deviation of the glutamate plus nitrate/glutamate gene expression ratio.

Table 3. Analysis of the *nasT* promoter by *lacZ* (β-galactosidase activity) gene fusion in *P. denitrificans* wild-type and *ntrB* and *ntrY* mutant strains.

	N-source			
Strain/construct	NH_4^+	NO_3^-	Glu	Glu + NO_3^-
WT/PnasT (native)	71 ± 5	14500 ± 143	11000 ± 120	15000 ± 152
WT/PnasT (mutated)*	50 ± 3	220 ± 14	53 ± 5	600 ± 25
ntrY/ PnasT (native)	n.d.	n.d.	11500 ± 115	15200 ± 135
ntrB/ PnasT (native)	n.d.	n.d.	10 ± 1	120 ± 4

* The base substitutions are specified in Table S2; n.d.: not determined.

REFERENCES

1. Richardson, D. J., Berks, B. C., Rusell, D. A., Spiro, S., and Taylor, C. J. (2001) Functional, biochemical and genetic diversity of prokaryotic nitrate reductases. Cell. Mol. Life Sci. **58**, 165-178
2. Gates, A. J., Luque-Almagro, V. M., Goddard, A. D., Ferguson, S. J., Roldán, M. D., and Richardson, D. J. (2011) A composite biochemical system for bacterial nitrate and nitrite assimilation as exemplified by *Paracoccus denitrificans.* Biochem. J. **435**, 743-753
3. Goddard, A. D., Bali, S., Mavridou, D. A., Luque-Almagro, V. M., Gates, A. J., Roldán, M. D., Newstead, S., Richardson, D. J., and Ferguson, S. J. (2017). The *Paracoccus denitrificans* NarK-like nitrate and nitrite transporters-probing nitrate uptake and nitrate/nitrite exchange mechanisms. Mol. Microbiol. **103**, 117-133
4. Shu, C. J., and Zhulin, I. B. (2002) ANTAR: an RNA-binding domain in transcription antitermination regulatory proteins. Trends Biochem. Sci. **27**, 3–5
5. Luque-Almagro, V. M., Lyall, V. J., Ferguson, S. J., Roldán, M. D., Richardson, D. J., and Gates, A. (2013) Nitrogen oxyanion-dependent dissociation of a two-component complex that regulates bacterial nitrate assimilation. J. Biol. Chem. **288**, 29692–29702
6. Waller, Z. A. E., Pinchbeck, B. J., Buguth, B. S., Meadows, T. J., Richardson, D. J., and Gates, A. J. (2016). Control of bacterial nitrate assimilation by stabilization of G-quadruplex DNA. Chem. Commun. **52**, 13511-13514
7. Moreno-Vivián, C., and Flores, E. (2007) Nitrate assimilation in Bacteria. In Biology of the Nitrogen Cycle. Bothe, H., S. J. Ferguson, W. E. and Newton (eds). Amsterdam: Elsevier, pp.263-282
8. Luque-Almagro, V. M., Gates, A. J., Moreno-Vivián, C., Ferguson, S. J., Richardson, D. J., and Roldán, M. D. (2011) Bacterial nitrate assimilation: gene distribution and regulation. Biochem. Soc. Trans. **39**, 1838-1843
9. Paz-Yepes J., Flores, E., and Herrero, A. (2003) Transcriptional effects of the signal transduction protein P_{II} (*glnB* gene product) on NtcA-dependent genes in *Synechococcus* sp. PCC 7942. FEBS Lett. **543**, 42-46
10. Forchhammer, K. (2004) Global carbon/nitrogen control by pII signal transduction in cyanoacteria: from signals to targets. FEMS Microbiol. Rev. **28**, 319-333
11. Flores, E., Frias, J. E., Rubio L. M., and Herrero, A. (2005) Photosynthetic nitrate assimilation in cyanobacteria. Photosynth. Res. **83**, 117-133
12. Kayumov, A., Heinrich, A., Sharipova, M., Lljinskaya, O., and Forchhammer, K. (2008) Inactivation of general transcription factor TnrA in *Bacillus subtilis* by proteolysis. Microbiology **154**, 2348-2355
13. Tiffert, Y., Supra, P., Wurm. R., Wohlleben, W., Wagner, R., and Reuther, J. (2008) The *Streptomyces coelicolor* GlnR regulon: identification of new GlnR targets and evidence for a central role of GlnR in nitrogen metabolism in actinomycetes. Mol. Microbiol. **67**, 861-880
14. Lin, J. T., and Stewart, V. (1996) Nitrate and nitrite-mediated transcription antitermination control of *nasF* (nitrate assimilation) operon expression in *Klebsiella pneumoniae* M5a1. J. Mol. Biol. **256**, 423-435
15. Chai, W., and Stewart, V. (1999) RNA sequence requirements for NasR-mediated, nitrate-responsive transcription antitermination of the *Klebsiella oxytoca* M5al *nasF* operon leader. J. Mol. Biol. **292**, 203-216

16. Boudes, M., Lazar, N., Graille, M., Durand, D., Gaidenko, T. A., Steward, V., and Tilbeurgh, H. (2012) The structure of the NasR transcription antiterminator reveals a one-componet system with a NIT nitrate receptor coupled to an ANTAR RNA-binding effector. Mol. Microbiol. **85**, 431-444
17. Gutiérrez, J. C., Ramos, F., Ortner, L., and Tortolero, M. (1995) *nasST*, two genes involved in the induction of the assimilatory nitrate-nitrite reductase operon (*nasAB)* of *Azotobacter vinelandii*. Mol. Microbiol. **18**, 579-591
18. Caballero, A., Esteve-Núnez, A., Zylstra, G. J., and Ramos, J. L. (2005) Assimilation of nitrogen from nitrite and trinitrotoluene in *Pseudomonas putida* JLR11. J. Bacteriol. **187**, 396-399
19. Toukdarian, A., and Kennedy, C. (1986) Regulation of nitrogen metabolism in *Azotobacter vinelandii*: isolation of *ntr* and *glnA* genes and construction of *ntr* mutants. EMBO J. **5**, 399-407
20. Wang, B., Pierson III, L. S., Rensing, C., Gunatilaka, M. K., and Kennedy. C. (2012) NasT-mediated antitermination plays an essential role in the regulation of the assimilatory nitrate reductase operon in *Azotobacter vinelandii*. Appl. Environ. Microbiol. **78**, 6558-6567
21. Swanson, R. V., Alex, L. A., and Simon, M. I. (1994) Histidine and aspartate phosphorylation: two-component systems and the limits of homology. Trends Biochem. Sci. **19**, 485-90
22. Sanders, D. A., Gillece-Castro, B. L., Burlingame, A. L., and Koshland, D. E., Jr. (1992) Phosphorylation site of NtrC, a protein phosphatase whose covalent intermediate activates transcription. J. Bacteriol. **174**, 5117–5122
23. Chen, P., and Reitzer, L. J. (1996) Active contribution of two domains to cooperative DNA binding of the enhancer-binding protein regulator I (NtrC) of *Escherichia coli*: stimulation by phosphorylation and the binding of ATP. J. Bacteriol. **177**, 2490-2496
24. Cullen, P. J., Bowman, W. C., and Kranz, R. G. (1996) In vitro reconstitution and characterization of the *Rhodobacter capsulatus* NtrB and NtrC two-component system. J. Biol. Chem. **271**, 6530–6536
25. Pawlowsky, K., Klosse, U., and the Bruijn, F. J. (1991). Characterization of a novel *Azorhizobium caulinodans* ORS571 two-component regulatory system, NtrY/NtrX, involved in nitrogen fixation metabolism. Mol. Gen. Genet. **231**, 124-138
26. Ishida, M. L., Assumpção, M. C., Machado, H. B., Benelli, E. M., de Souza, E. M., and Pedrosa, F. O. (2002) Identification and characterization of the two-component NtrY/NtrX regulatory system in *Azospirillum brasilense*. Braz. J. Med. Biol. Res. **35**, 651-661
27. Assumpção, M. C., de Souza, E. M., Yates, M. G., de Oliviera-Pedrosa, F., and Machado-Benelli, E. (2007) Purificacion and charcterization of *Azospirillum brasilense* N-truncated NtrX protein. Prot. Express. Purif. **53**, 302-308
28. Bonato, P., Alves, L. R., Osaki, J. H., Rigo, L. U., Pedrosa, F. O., de Souza, E. M., Zhang, N., Schumacher, J., Buck, M., Wassem, R., and Chubatsu1, L. S. (2016). The NtrY/NtrX two-component system is involved in controlling nitrate assimilation in *Herbaspirillum seropedicae* strain SmR1. FEBS J. **283**, 3919-3930
29. Drepper, T., Wiethaus, J., Giaourakis, D., Groβ, S., Schubert, B., Vogt, M., Wiencek, Y., McEwan, A. G., and Masepohl, B. (2006) Cross-talk towards response regulator NtrC controlling nitrogen metabolism in *Rhodobacter capsulatus*. FEMS Microbiol. Lett. **258**, 210-256

30. Carrica, M. C., Fernandez, I., Martí, M. A., Paris, G., and Goldbaum, F. A. (2012) The NtrY/X two-component system of *Brucella* spp. acts as a redox sensor and regulates the expression of nitrogen respiration enzymes. Mol. Microbiol. **85**, 39-50
31. Roop II, R. M., and Caswell, C. C. (2012) Redox-responsive regulation of denitrification genes in *Brucella*. Mol. Microbiol. **85**, 5-7
32. Sambrook, J., Fritsch, E.F., and Maniatis, T. (1989) Molecular cloning. In A laboratory manual, 2nd edn. New York: Cold Spring Harbor Laboratory, Cold Spring Harbor
33. Robertson, L. A., and Kuenen, J. G. (1983) *Thiosphaera pantotropha* gen. nov. sp. nov., a facultatively anaerobic, facultatively autotrophic sulphur bacterium. J. Gen. Microbiol. **129**, 2847-2855
34. Shakir, F. K., Audilet, D., Drake, A. J. III, and Shakir, K. M. M. (1994) A rapid protein determination by modification of the Lowry procedure. Anal. Biochem. **216**, 232-233
35. Snell, F. D., and Snell, C. T. (1949) Nitrites. In Colorimetric methods of analysis. Snell, F. D., and C. T. Snell (eds). New York: van Nostrand, pp.802-807
36. Miller, J. M. **(**1972) In Experiments in molecular genetics. Miller, J. (ed). New York: Cold Spring Harbor Laboratory Press, pp.171-224
37. Alston, M. J., Seers, J., Hinton, J. C., and Lucchini, S. (2010) BABAR: an R package to simplify the normalisation of common reference design microarray-based transcriptomic datasets. BMC Bioinformatics **11**, 73
38. Untergasser, A., Nijveen, H., Rao, X., Bisseling, T., Geurts, R., and Leunissen, J. A. (2007) Primer3Plus, an enhanced web interface to Primer3. Nucleic Acids Res **35**, W71-74
39. Pfaffl, M. W. (2001) A new mathematical model for relative quantification in real-time RT-PCR. Nucleic Acids Res. **29**, E45
40. Luque-Almagro, V. M., Huertas, M. J., Roldán M. D., Moreno-Vivián, C., Martínez-Luque, M., Blasco, R., and Castillo, F. (2007) The cyanotrophic bacterium *Pseudomonas pseudoalcaligenes* CECT5344 responds to cyanide by defence mechanism against iron deprivation, oxidative damage and nitrogen stress. Environ. Microbiol. **9**, 1541-1549
41. Sánchez, C., Itakura, M., Okubo, T., Matsumoto, T., Yoshikawa, H., Gotoh, A., Hidaka, M., Uchida, T., and Minamisawa, K. (2014) The nitrate-sensing NasST system regulates nitrous oxide reductase and periplasmic nitrate reductase in *Bradyrhizobium japonicum*. Environ. Microbiol. **16**, 3263-3274
42. Pino, C., Olmo-Mira, M. F., Cabello, P., Martínez-Luque, M., Castillo, F., Roldán, M. D., and Moreno-Vivián, C. (2006) The assimilatory nitrate reduction system of the phototrophic bacterium *Rhodobacter capsulatus* E1F1. Biochem. Soc. Trans. **34**, 127-129
43. Wang, B., Rensing, C., Pierson III, L. S., Zhao, H., and Kennedy, C. (2014) Translational coupling of *nasST* expression in *Azotobacter vinelandii* prevents overexpression of the *nasT* gene. FEMS Microbiol. Lett. **361**, 123-130
44. Sun, J., Peng, X., van Impe, J., and Vanderleyden J. (2000) The *ntrB* and *ntrC* genes are involved in the regulation of poly-3-hydroxybutyrate biosynthesis by ammonia in *Azospirillum brasilense* Sp7. Appl. Environ. Microbiol. **66**, 11-117

FIGURE LEGENDS

Figure 1. Transcriptomic and proteomic analysis of aerobically cells grown with nitrate or ammonium as nitrogen source. (A) Heat map from DNA microarrays analyses of *P. denitrificans* PD1222 grown aerobically with either ammonium or nitrate as the sole nitrogen source. Colours indicate $\log_2$ of normalised expression values in either condition. Genes were selected based on at least 2-fold change in expression with *p*-values ≤ 0.05. A total of 74 genes were up-regulated more than 2-fold under nitrate assimilation conditions, whereas nine genes were down-regulated more than 2-fold under these conditions. (**B**) 2D-PAGE analysis of *P. denitrificans* PD1222 soluble fractions from cells grown aerobically with ammonium or nitrate (10 mM each) as the sole nitrogen source. Spots present or absent in gels are highlighted by black or white triangles, respectively. The presented gels are representative of three independent replicants.

Figure 2. Analysis by RT-PCR and qPCR of the *P. denitrificans* nitrate assimilation *nas* genes. (**A**) The *nas* gene cluster of *P. denitrificans* and the location of the oligonucleotides used in this study are shown. (**B**) RT-PCR reactions with RNA from the wild-type strain of *P. denitrificans* grown in the presence of different N-sources. To isolate RNA, cells were cultured in minimal medium with different N-sources as described in Materials and Methods section and harvested at an A_{600} of about 0.4. The *rpoB* gene was used as housekeeping. -/+, without/with reverse transcriptase (**C**) RT-qPCR analysis of the *nasT*, *nasS* and *nasA* genes from cells grown with different nitrogen sources. Error bars represent standard deviation calculated from the results of three independent experiments.

Figure 3. Characterization of the wild-type strain and the *nasT* and *nasS* mutants of *P. denitrificans* with different nitrogen sources. (**A**) NADH-dependent nitrate reductase activity and NasG polypeptide detection by 2D-PAGE analysis in the wild-type strain of *P. denitrificans*. The 2D-PAGE analyses were carried out in cytoplasmic fraction from cells grown with different nitrogen sources obtained by subcellular fractionations as indicated in Materials and Methods. The different nitrogen sources were nitrate, ammonium, ammonium plus nitrate, glutamate or glutamate plus nitrate (10 mM each). Isoelectric focusing was performed from IPG strips range 4-7 and second dimension was carried out onto 12% polyacrylamide gels. The nitrate reductase activity (NR) was assayed in cytoplasmic fractions and was undetectable with glutamate or ammonium as N-source, and expressed as nmol NO_2^- formed min^{-1} mg^{-1} (n.d, not detected). (**B**) RT-PCR analysis of structural *nas* genes in the wild-type and *nasT* and *nasS* mutant strains of *P. denitrificans*. To isolate RNA, wild-type and *nasT* and *nasS* strains were cultured in minimal medium with different N-sources as described in Materials and Methods section and harvested at an A_{600} of about 0.4. The *rpoB* gene was used as housekeeping. -/+, without/with reverse transcriptase. (**C**) NasG polypeptide detection by 2D-PAGE analysis and NADH-nitrate reductase activity in cytoplasmic fractions from *nasT* and *nasS* mutant strains of *P. denitrificans*. The 2D-PAGE analysis and the NR activity assays were performed as indicated in (A) for the wild-type strain.

Figure 4. Analysis of the *nasA* leader region of *P. denitrificans*. (**A**) Intergenic *nasS-nasA* region from *P. denitrificans*. (**B**) Expression of the transcriptional P_{nasA}-*lacZ* fusions and effect of mutations within the leader sequence on *nasA-lacZ* expression in cells grown with ammonium or nitrate (10 mM each). The β-galactosidase activity was

measured when the A_{600} was about 1.0 and it was represented as Miller units (M.U.). Control represents the wild type (native) construction from -321 to +71 nucleotides of the *nasS-nasA* intergenic region. HI and HII represent the P_{nasA}-*lacZ* constructions with 3 bp mutations in each hairpin. (**C**) Growth curves with nitrate as sole nitrogen source of the *P. denitrificans* wild-type strain and the mutants in the *nasT* gene and the *cis*-acting NasT binding region (hairpin I, HI).

Figure 5. Characterization of the *ntrB*, *ntrY* and double *ntrB*/*ntrY* mutant strains of *P. denitrificans* in media with nitrate. (**A**) Growth-curves of *P. denitrificans* wild-type strain (●), and *ntrB* (■), *ntrY* (▲) and double *ntrB*/*ntrY* (◆) mutants with 10 mM nitrate as nitrogen source. (**B**) RT-qPCR analysis of the regulatory genes *nasT*, *nasS*, *ntrB* and *ntrY* and the structural *nasA* gene in the wild-type strains and the *ntrB* mutant strains of *P. denitrificans* grown with 10 mM nitrate as N-source. The oligonucleotides used in the qPCR analysis for the *ntrB* and *ntrY* genes hybridized upstream the mutation site. Represented data were normalized by using the *rpoB* and *dnaN* genes as housekeeping (Table S2). Error bars represent standard deviation calculated from the results of three independent experiments.

Figure 6. Proposed model of the nitrate assimilation regulation in *P. denitrificans*. The model describes the regulatory cascade controlling expression of nitrate assimilation *nas* genes by the *ntrBCYX* gene cluster in response to ammonium availability and by the *nasTS* genes for nitrate control. Levels 1 and 2 include regulatory mechanisms that control transcription of the *nas* genes, whereas level 3 involves a control on the translation of the Nas proteins. A circle with a plus symbol means activation of the transcription and a circle with the capital letter A indicates transcription antitermination.

A

Gene ID	Name	NH_4^+	NO_3^-	Function / Annotation
281	*ehuB*			ABC transporter ectoine binding protein
286	*eutC*			Ectoine utilisation protein
288	*eutE*			Succinylglutamate desuccinylase/aspartoacylase
488	*gltB*			Glutamate synthase Large Subunit (GOGAT)
489	---			conserved hypothetical protein
490	*gltD*			Glutamate synthase Small Subunit (GOGAT)
552	---			Putative inner membrane protein
553	---			hypothetical protein
556	---			hypothetical protein
567	*sdhC*			succinate dehydrogenase subunit C
607	*dppB*			Peptide/nickel/opine ABC-transporter permease
608	*dppA*			Peptide/nickel/opine ABC-transporter binding protein
794	*btzB*			Glu/Asp ABC-transporter Permease
795	*btzC*			Glu/Asp ABC-transporter Permease
796	*btzD*			Glu/Asp ABC-transporter ATP-binding protein
823	---			protein of unknown function DUF404
824	---			protein of unknown function DUF403
825	---			transglutaminase, N-terminal domain protein
945	*proX*			Glycine/betaine ABC-transporter binding protein
1205	*ureG*			Urease cobalamin synthesis protein
1206	*ureE*			Urease accessory protein
1207	*ureF*			Urease accessory protein
1208	*ureC*			Urease α-subunit
1209	*ureB*			Urease β-subunit
1210	*ureJ*			Urease accessory protein
1211	*ureA*			Urease γ-subunit
1212	*ureD*			Urease accessory protein
1248	*dpdA*			Peptide/nickel/opine ABC-transporter binding protein
1508	---			Lytic transglycosylase, catalytic
2032	*amtB*			Ammonium transporter AmtB
2149	*potI*			Polyamine ABC transporter permease
2150	*potH*			Polyamine ABC transporter permease
2151	*potD*			Polyamine periplasmic binding protein
2152	*potF*			Polyamine periplasmic binding protein
2153	*potG*			ABC transporter ATP-binding protein
2472	*ugpB*			Carbohydrate ABC transporter binding protein
2543	---			hypothetical protein
2610	*bhuA*			Hemin TonB-dependent transporter
2961	*icd*			isocitrate dehydrogenase (NADP)
3349	*hns*			nucleoid protein H-NS
3461	*potB*			Polyamine ABC-transporter permease
3462	*potC*			Polyamine ABC-transporter permease

Gene ID	Name	NH_4^+	NO_3^-	Function / Annotation
3705	*argT*			Amino acid ABC transporter substrate-binding protein
3928	*braE*			Branched-chain amino acid ABC transporter permease
3929	*braD*			Branched-chain amino acid ABC transporter permease
3930	*braG*			ABC transporter ATP-binding protein
3931	*braF*			ABC transporter ATP-binding protein
3932	*braC*			Branched-chain amino acid binding protein
4017	*urtA*			Urea-binding protein
4018	*urtB*			Urea ABC transporter permease
4019	*urtC*			Urea ABC transporter permease
4020	*urtD*			Urea ABC transporter ATP-binding protein
4021	*urtE*			Urea ABC transporter ATP-binding protein
4110	*citE*			Citrate lyase
4129	*ntrC*			Two-component σ54 specific transcriptional regulator
4130	*ntrB*			Nitrogen specific signal transduction histidine kinase
4131	---			hypothetical protein
4234	*narJ*			Respiratory nitrate reductase chaperone (NarJ)
4236	*narG*			Respiratory nitrate reductase alpha subunit (NarG)
4449	*nasC*			Assimilatory nitrate reductase (NasC)
4450	*nasH*			Nitrite transporter (NasH)
4451	*nasG*			Assimilatory nitrite reductase small subunit (NasG)
4452	*nasB*			Assimilatory nitrite reductase large subunit (NasB)
4453	*nasA*			Nitrate/nitrite transporter (NasA)
4454	*nasS*			Putative nitrate binding protein
4455	*nasT*			Response regulator reciever and ANTAR domain protein
4461	*glnB*			nitrogen regulatory protein P-II
4462	*glnA*			Glutamine synthetase (GS)
4619	*dctP*			TRAP dicarboxylate transporter binding protein
4620	*dctQ*			TRAP dicarboxylate transporter small membrane protein
4621	*dctM*			TRAP dicarboxylate transporter large membrane protein
4864	*hisJ*			Amino acid ABC transporter binding protein
4888	*proX*			Glycine/betaine ABC-transporter binding protein
5095	*livK*			Branched chain amino acid ABC transporter binding protein

317	---			hypothetical protein
623	---			protein of unknown function DUF1127
650	*matE*			MATE efflux family protein
1552	---			conserved hypothetical protein
3196	*trbB*			conjugal transfer protein TrbB
3872	*gdhA*			Glutamate dehydrogenase (GDH)
4121	*dctQ*			TRAP dicarboxylate transporter small membrane protein
4718	---			hypothetical protein
4725	---			conserved hypothetical protein

-3 -2 -1 0 1 2 3 4 5 6 7

B

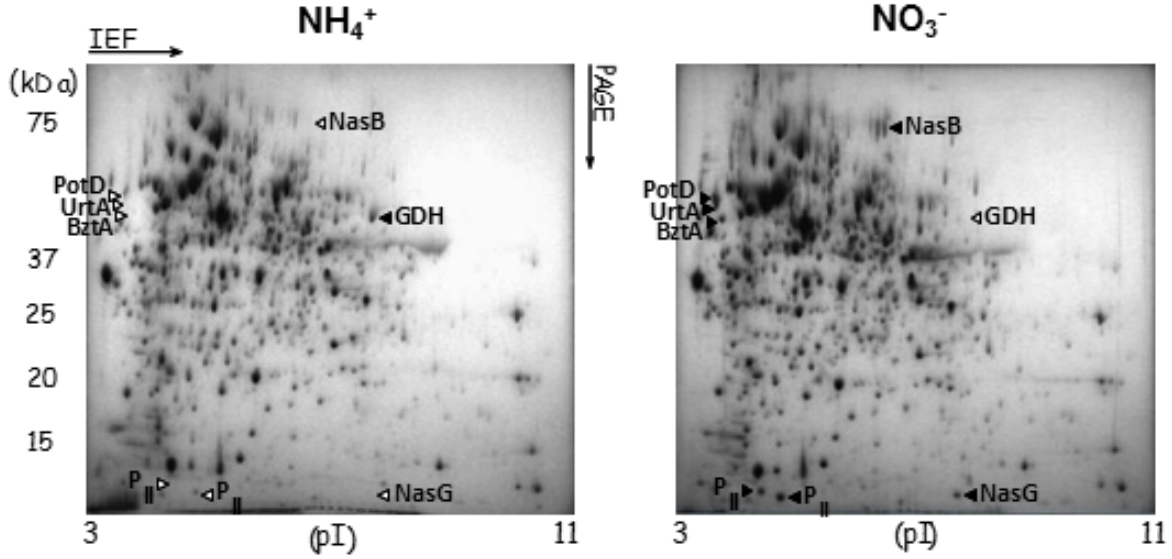

Figure 1

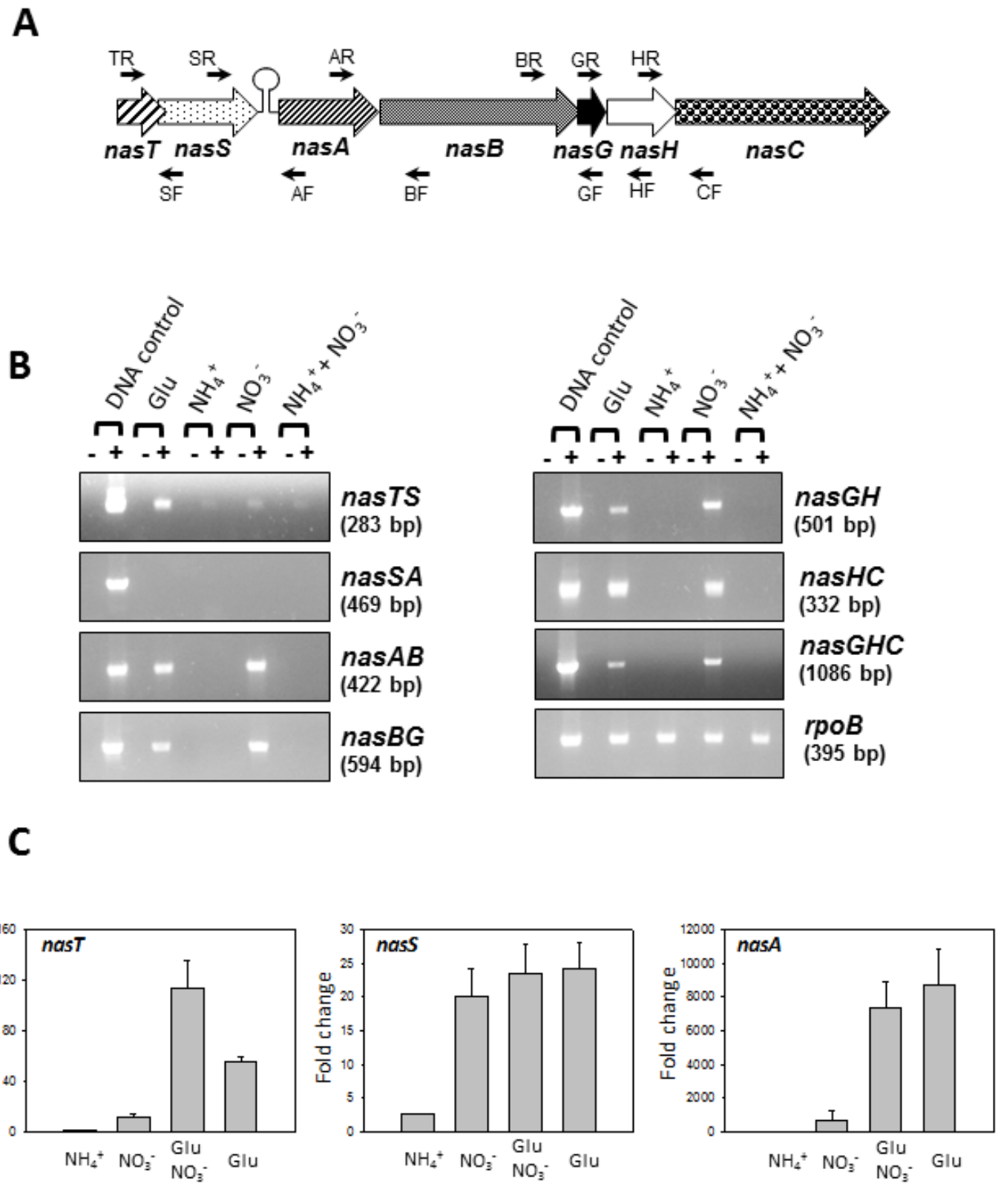
A
TR
SR
AR
BR
GR
HR
nasT
nasS
nasA
nasB
nasG
nasH
nasC
SF
AF
BF
GF
HF
CF
B
DNA control
Glu
NH4+
NO3-
NH4+ + NO3-
nasTS
(283 bp)
nasSA
(469 bp)
nasAB
(422 bp)
nasBG
(594 bp)
nasGH
(501 bp)
nasHC
(332 bp)
nasGHC
(1086 bp)
rpoB
(395 bp)
C
nasT
nasS
nasA
Fold change
NH4+
NO3-
Glu
Glu NO3-

Figure 2

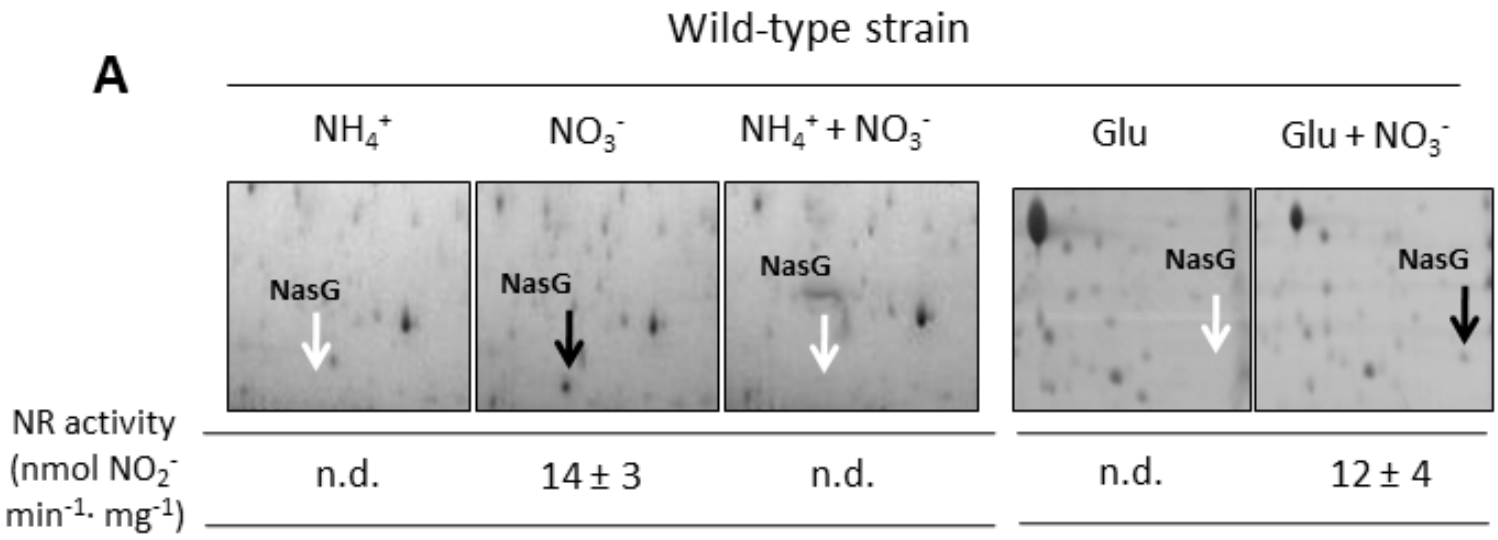
A
Wild-type strain
NH_4^+
NO_3^-
$NH_4^+ + NO_3^-$
Glu
Glu + NO_3^-
NasG
NasG
NasG
NasG
NasG
NR activity (nmol NO_2^- min^{-1}· mg^{-1})
n.d.
14 ± 3
n.d.
n.d.
12 ± 4

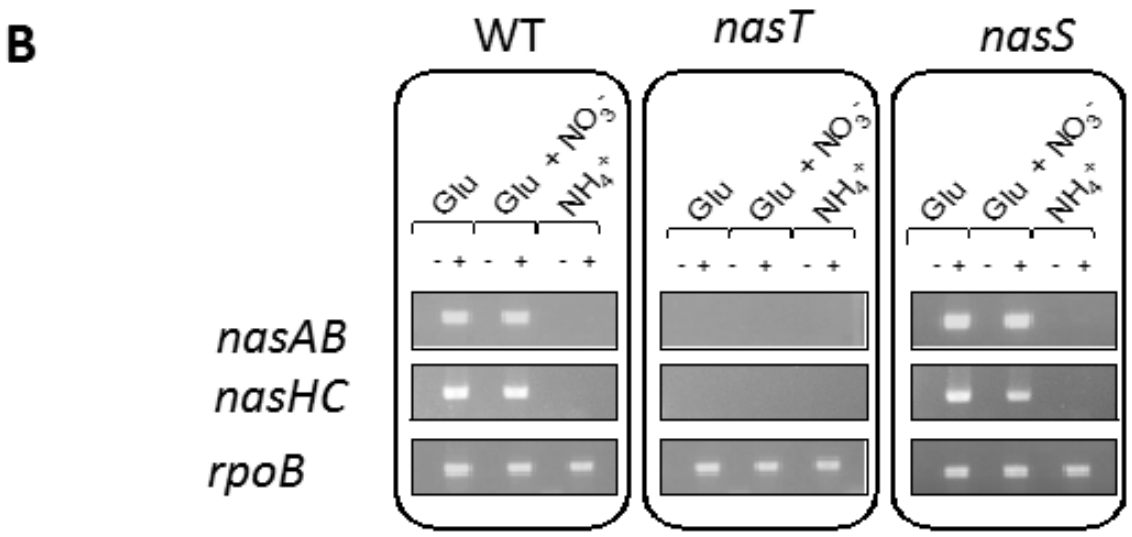
B
WT
nasT
nasS
Glu
Glu + NO_3^-
NH_4^+
nasAB
nasHC
rpoB

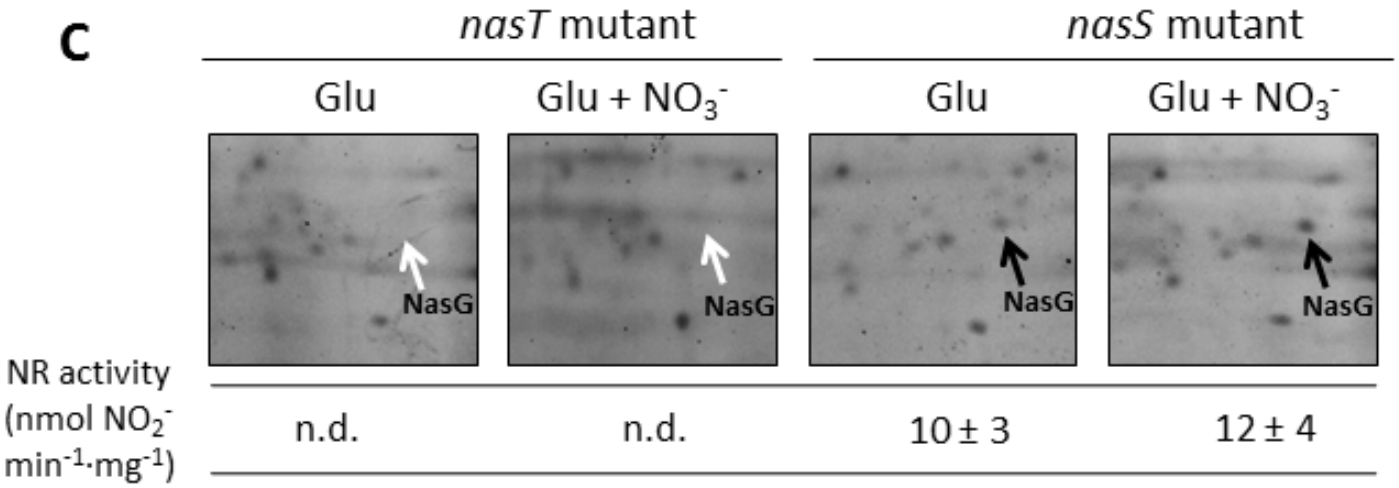
C
nasT mutant
nasS mutant
Glu
Glu + NO_3^-
Glu
Glu + NO_3^-
NasG
NasG
NasG
NasG
NR activity (nmol NO_2^- min^{-1}·mg^{-1})
n.d.
n.d.
10 ± 3
12 ± 4

Figure 3

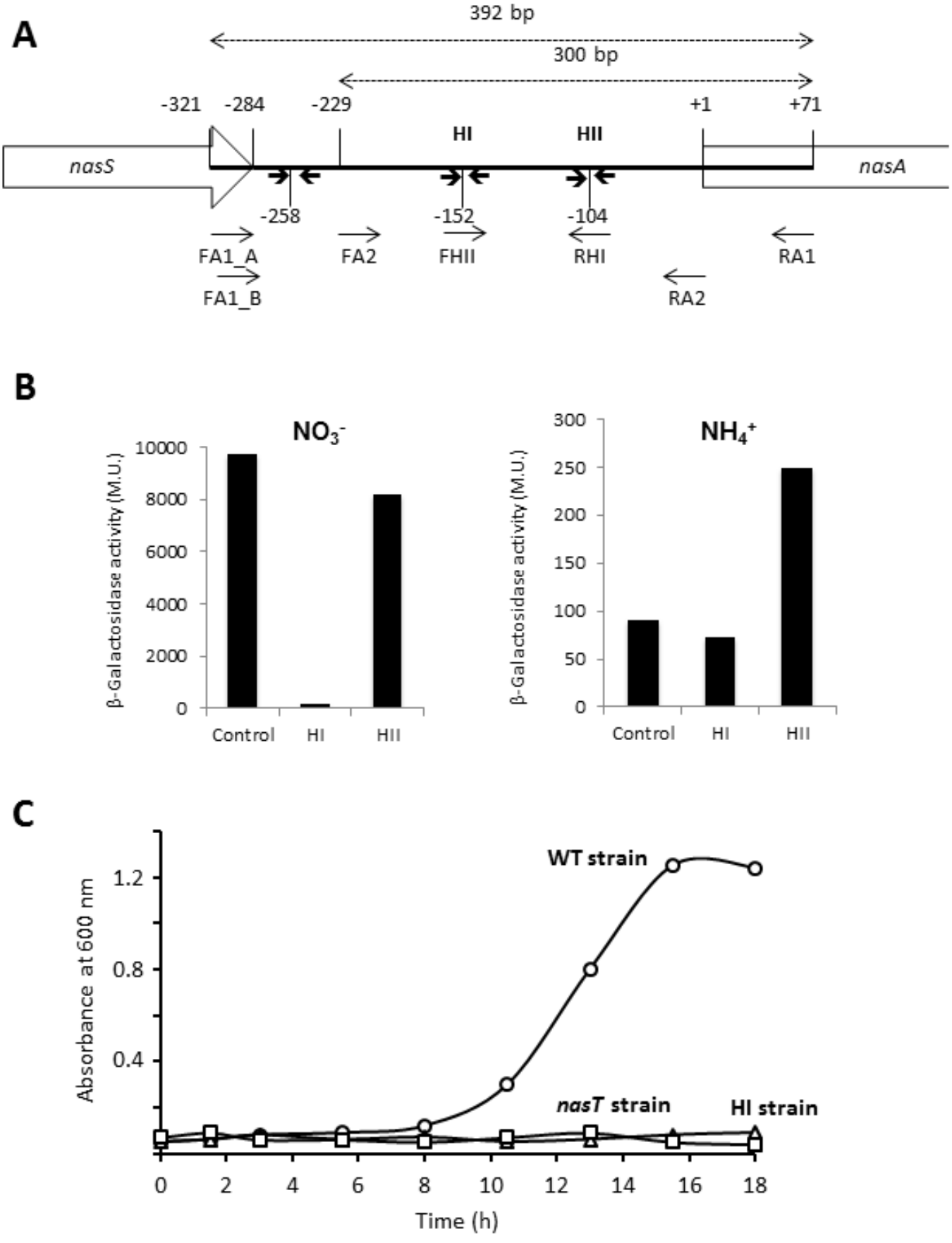
A
392 bp
300 bp
-321
-284
-229
+1
+71
HI
HII
nasS
nasA
-258
-152
-104
FA1_A
FA1_B
FA2
FHII
RHI
RA1
RA2
B
NO3-
NH4+
β-Galactosidase activity (M.U.)
10000
8000
6000
4000
2000
0
300
250
200
150
100
50
Control
HI
HII
C
WT strain
nasT strain
HI strain
Absorbance at 600 nm
1.2
0.8
0.4
0
2
4
6
8
10
12
14
16
18
Time (h)

Figure 4

A

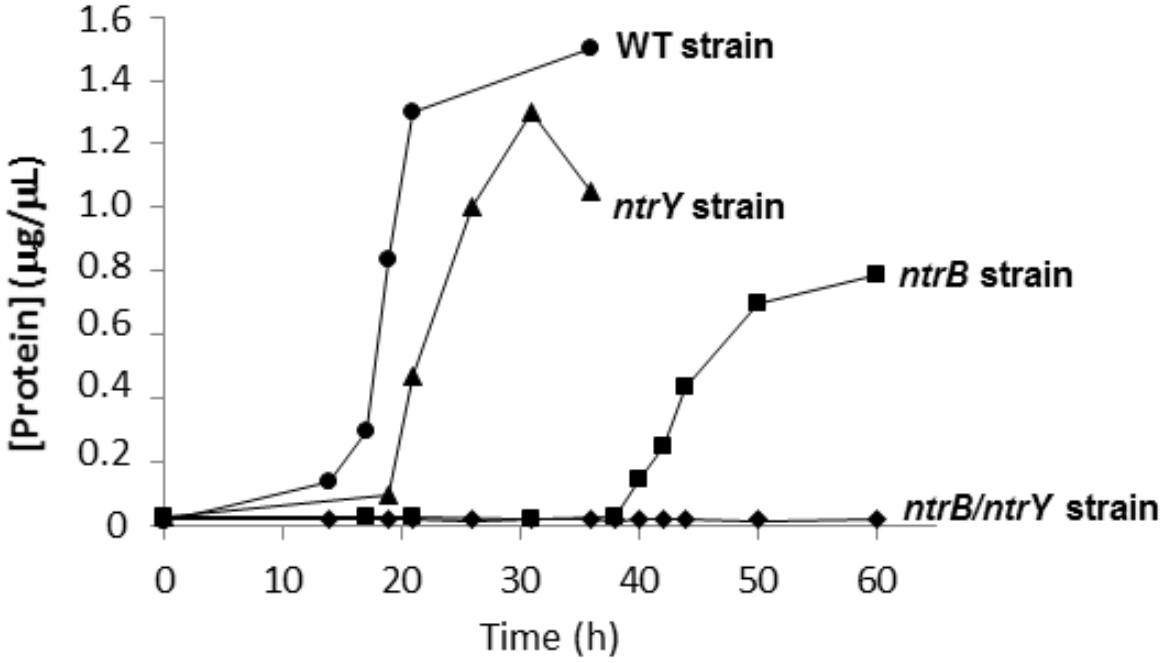
1.6
1.4
1.2
1.0
0.8
0.6
0.4
0.2
0
[Protein] (µg/µL)
WT strain
ntrY strain
ntrB strain
ntrB/ntrY strain
0
10
20
30
40
50
60
Time (h)

B

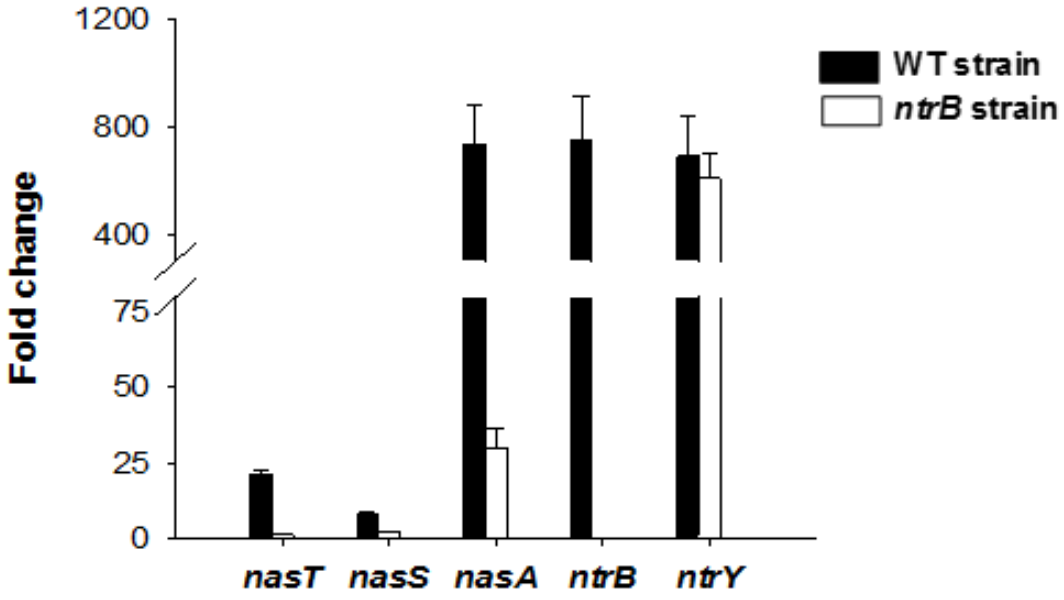
1200
800
400
75
50
25
0
Fold change
WT strain
ntrB strain
nasT
nasS
nasA
ntrB
ntrY

Figure 5

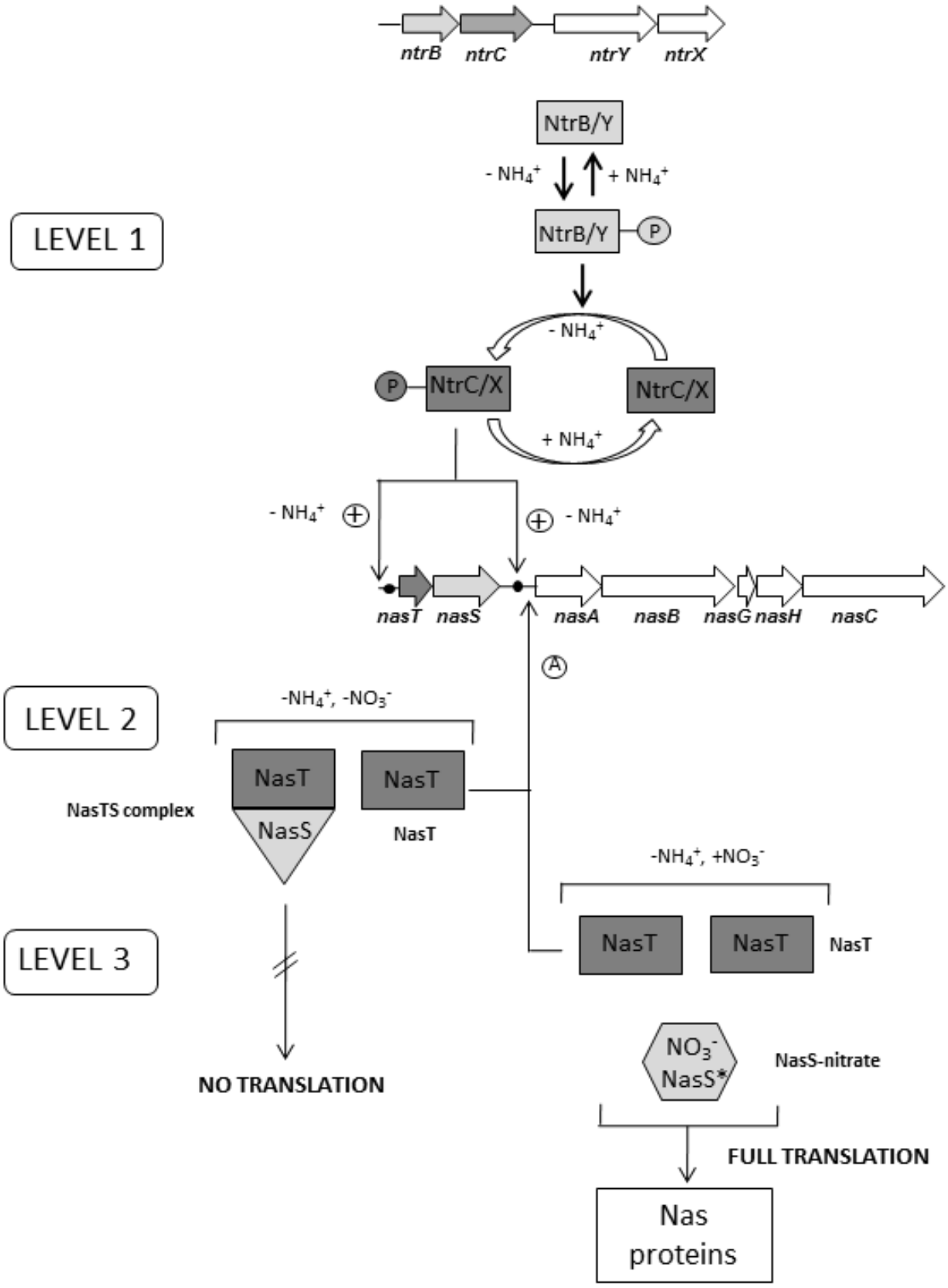
ntrB
ntrC
ntrY
ntrX
NtrB/Y
- NH4+
+ NH4+
NtrB/Y
P
LEVEL 1
- NH4+
P
NtrC/X
NtrC/X
+ NH4+
- NH4+
- NH4+
nasT
nasS
nasA
nasB
nasG
nasH
nasC
A
LEVEL 2
-NH4+, -NO3-
NasT
NasS
NasT
NasTS complex
NasT
LEVEL 3
-NH4+, +NO3-
NasT
NasT
NasT
NO TRANSLATION
NO3-
NasS*
NasS-nitrate
FULL TRANSLATION
Nas
proteins

Figure 6

Table S1. Bacterial strains and plasmids used in this study.

Strain or plasmid	Genotype and description	Source or reference
***Paracoccus denitrificans* PD1222**		
Wild-type	Sp^R, Rif^R, enhanced conjugation frequencies	[1]
nasT	*nasT*Δ::Sm^R	[2]
nasS	*nasS*Δ::Km^R	[2]
ntrB	*ntrB*Δ::Sm^R	This work
ntrY	*ntrY*Δ::Km^R	This work
ntrB/*ntrY*	*ntrB*Δ::Sm^R/*ntrY*Δ::Km^R	This work
HI (hairpin I)	Unmarked mutant	This work
Escherichia coli		
DH5α	*deoR endA1 gyrA96 hsdR17*(r_k^- m_k^+) *recA1 relA1 supE44 thi-1* Δ*(lacZYA-argFV169) Ø80 δlacZ*ΔM15 F^- λ^-	[3]
pRK2013	Km^R, Tra^+ (pRK2013 encoded) helper strain	[4]
Plasmids		
pUC18	Amp^R, cloning vector	[5]
pGEM-Teasy	Amp^R, cloning vector	Promega (USA)
pGEM-T	Amp^R, cloning vector	Promega (USA)
pSparkII	Amp^R, cloning vector	Canvax (Spain)
pSUP202	Amp^R, Tet^R, Cm^R, Mob^-, mobilizable suicide vector	[6]
pSUP202*	pSUP202::Km-ΔTet, mobilizable suicide vector	[7]
pSUP2021	pSUP202::Tn*5*, source of Km^R cassette	[6]
pK18*mobsacB*	Gene knockout vector, Km^R	[8]
pSRA2	Amp^R, Sp^R, Sm^R, source of Sm^R cassette	[9]
pMP220	Promoter probe vector, *lacZ* gene, IncP1 Tc^R	[10]
pMP220-*P*nasA	pMP220-based transcriptional fusion spanning the intergenic region between *nasS* and *nasA* (Tet^R)	This work
pMP220-*P*nasA1	pMP220-based transcriptional fusion spanning the intergenic region between *nasS* and *nasA* containing the hairpin I mutated (Tet^R)	This work
pMP220-*P*nasA2	pMP220-based transcriptional fusion spanning the intergenic region between *nasS* and *nasA* containing the hairpin II mutated (Tet^R)	This work
pMP220-*P*nasT	pMP220-based transcriptional fusion spanning the *nasT* leader region (Tet^R)	This work
pMP220-*P*nasT1	pMP220-based transcriptional fusion spanning the *nasT* leader region and containing the	This work

	NtrC-binding site mutated (Tet^R)	

Table S2. Oligonucleotide primers used in this study.

Primer	Sequence (5'→ 3')[a]	Used for
ntrB1-HB (*Hin*dIII-*Bam*HI)	CCCAAGCTTACGAATTCTCGCCAATGGCGACGTGGTGGATGCGGCCTCGC	*ntrB* mutagenesis
ntrB2-B (*Bam*HI)	CGGGATCCCAGGATCGCGCCGAGCCGGGGCACGATG	*ntrB* mutagenesis
ntrB3-B (*Bam*HI)	CCCTGCGGATCCAGATCGAGGACGACGGCCC	*ntrB* mutagenesis
ntrB4-K (*Kpn*I)	ACGGGGTACCCGAAGGGCTTGGGCAGGTAGTCGAAGGC	*ntrB* mutagenesis
ntrY1-A (*Aat*II)	GATGACGTCGCGAGAGTCGCTGAACGGCCACAGAA	*ntrY* mutagenesis
ntrY2-B (*Bam*HI)	CGCGGATCCCGAGGTCGAAACCACCTGCTGCACCC	*ntrY* mutagenesis
ntrY3-B (*Bam*HI)	GCCGGATCCCTGGAGGGCTATGTGGTGGCGCTGGA	*ntrY* mutagenesis
ntrY4-E (*Eco*RI)	GCCGAATTCCTCGGGGGCATCGGTCAGCATCAGGC	*ntrY* mutagenesis
PTF	CGCCACGCCGCATAATGGTCGAAGGGATAGT	*nasT*::*lacZ* fusion
PTR	GCGAGGGATTGGCCAGGTCGATCAGCA	*nasT*::*lacZ* fusion
PTNtrR	GCGGCGCTGCCCATGGTTCGGTAGGCG	*nasT*::*lacZ* fusion
PTNtrR_Mut	GCGGCGCT***AT***(GC)CC***C***(A)TGGTTCGGTAGGCG	Mutated *nasT* promoter::*lacZ* fusion
PTNtrF	CGCCTACCGAACCATGGGCAGCGCCGC	*nasT*::*lacZ* fusion
PTNtrF_Mut	CGCCTACCGAACCA***G***(T)GG***AT***(CG)AGCGCCGC	Mutated and native *nasT* promoter::*lacZ* fusion
FA1_A	CGACGGCACCATCTTCGA	*nasA*::*lacZ* fusion
RA1	GTAAAGGCGAAGGTCGAGAG	Mutated *nasA* promoter::*lacZ* fusion
RA1-S (*Sph*I)	TAGCATGCGTAAAGGCGAAGGTCGAGAG	Mutated *nasA* promoter ::*lacZ* fusion
FA1_B-P (*Pst*I)	ATCTGCAGACGGCACCATCTTCGAACCACC	Mutated *nasA* promoter (hairpin I)::*lacZ* fusion
RHI-A (*Asc*I)	GCCGGTGGCGCGCCGTT***CG***(GC)G***G***(C)CGGGCCAT	Mutated *nasA* promoter (haipin I)::*lacZ* fusion

FHII-A (*Asc*I)	AACGGCGCGCCACCGGCCCGCTCGCAATGATGCGGCAC GGAT***A***(T)C***GG***(CC)GCGA	Mutated *nasA* promoter (haipin II)::*lacZ* fusion
AIF1 (*Eco*RI)	AAGAATTCGCGAATATCTGGACCTGCCGGCGGAA	Unmarked hairpin I mutant
AIR1a	ATGGGATCAGACTGGGTCAGGACGCA	Unmarked hairpin I mutant
AIF2 (*Sal*I)	AAGTCGACCGCTCGCAATGATGCGGCACGGATTC	Unmarked hairpin I mutant
AIR2 (*Hin*dIII)	TTAAGCTTCATTGCCGGTGCCGAAGATGCCCAAC	Unmarked hairpin I mutant
nasTR	GATGCGGCCATCGCACGCTTTCACA	RT-PCR
nasSF	GCGGCGTCGATCAGCGGCACATAGC	RT-PCR
nasSR	GCGATGGCGCATTTCCGCACCGATCTTTACC	RT-PCR
nasAF	ATGCGTTGCTGATGGCGAAGGCTGTCGGAAA	RT-PCR
nasAR	CTGGGCAAGGCGGCCGTCTACAAGCACAT	RT-PCR
nasBF	CCCGACAGGACCGGCGACAGCATCAG	RT-PCR
nasBR	TGGTCTGCGTCGACAGCGGCTACCAGATCAG	RT-PCR
nasGF	GCGGTGCCCGAGTTCATGTCGAACACCCAGTT	RT-PCR
nasGR	CTGCCCGCTGCACAACTGGGTGTTCGACATGA	RT-PCR
nasHF	GCGAAATTGCCGCAAAAGACCAGGCCCCAGTT	RT-PCR
nasHR	ATCCTGATCTTCTTCTACATGGGTTTCGAGCATT	RT-PCR
nasCF	CGTCGCCAGCACGCCGCAGCCCACGCCGCAATA	RT-PCR
RT-RpoB5′	TTTGTCGCGAAAGACATCATCAACGAGCAGAC	RT-PCR (housekeeping)
RT-RpoB3′	TGGGTATCCGGCGCATCCAGGTCAAGG	RT-PCR (housekeeping)
RT-A5′	GATGTTCGTGGACCGCTCGGATGAG	qPCR (*nasT* gene)
RT-A3′	GGAACATGTGAAAGCGTGCGATGGC	qPCR (*nasT* gene)
RT-K5′	GGACGAGCCCGAGAACCGC	qPCR (*nasS* gene)
RT-K3′	CGGCGTGGAAGGCGATGAA	qPCR (*nasS* gene)
RT-C5′	GCGGTGATGTATGCGACCTTCATCG	qPCR (*nasA* gene)
RT-C3′	GCTGGGGATGTGCTTGTAGACGGC	qPCR (*nasA* gene)

RT-H5′	GCGACGTTCATCCGACCCATTACG	qPCR (*rpoB*-housekeeping)
RT-H3′	TGCCCTCGACCACCTTGCGGTAGG	qPCR (*rpoB*-housekeeping)
dnaN-1F′	CATGTCGTGGGTCAGCATAC	qPCR (*dnaN*-housekeeping)
dnaN-1R′	CTCGCGACCATGCATATAGA	qPCR (*dnaN*-housekeeping)
ntrB10	GCCATCATGGGCGAGGTTTTCGAGC	qPCR
ntrB11	CGGGGCGGGATTCCAGTGCGAT	qPCR
ntrY4	CGGTGAATATCGGGCTGGAGGGCTGG	qPCR
ntrY5	TGGCGTCGTTGGTCAAGTCTCGGCG	qPCR
nasT2F	TCGATCGTCGTCATCGAAT	qPCR to verify microarrays
nasT2R	GGTTTCTTCCGAGATGATGC	qPCR to verify microarrays
nasS2F	CTGGACCTGGTGATGTTCCT	qPCR to verify microarrays
nasS2R	ATCGCGAAAGTCGAAATCAT	qPCR to verify microarrays
nasA1F	CCTGACGCAGGTCTATGGTT	qPCR to verify microarrays
nasA1R	GACGATGAAGGTCGCATACA	qPCR to verify microarrays
nasB2F	TCTGGACCGGCCCTATAAAT	qPCR to verify microarrays
nasB2R	CGATAGACCGACTGGCTGAT	qPCR to verify microarrays
nasG1F	GTCTTTGCGCTGGACGAC	qPCR to verify microarrays
nasG1R	ATGTCGAACACCCAGTTGTG	qPCR to verify microarrays
nasH1F	TCATGTGCAACTGGATGGTT	qPCR to verify microarrays
nasH1R	CATGTTCACGATGGAATGCT	qPCR to verify microarrays
nasC1F	CTATGTCGCCAACAAGCTGA	qPCR to verify microarrays

nasC1R	CCAGCTCCAGATCCTCGTAG	qPCR to verify microarrays
ntrB10	GCCATCATGGGCGACGGTTTTCGAGC	qPCR to verify microarrays
ntrB11	CGGGGCGGGATTCCAGTGCGAT	qPCR to verify microarrays
ntrC1F	ACCGCTATTTCGACCTGCAT	qPCR to verify microarrays
ntrC1R	GGTTTATGCCCAGAAGATCG	qPCR to verify microarrays
GIDH1F	ACGGCAACACCTATTTCACC	qPCR to verify microarrays
GIDH1R	ATTCCTGCACCTTCTCGATG	qPCR to verify microarrays

[a]Enzyme restriction sites are underlined. Bases changed are marked in bold and italics and native bases are in brackets.

A

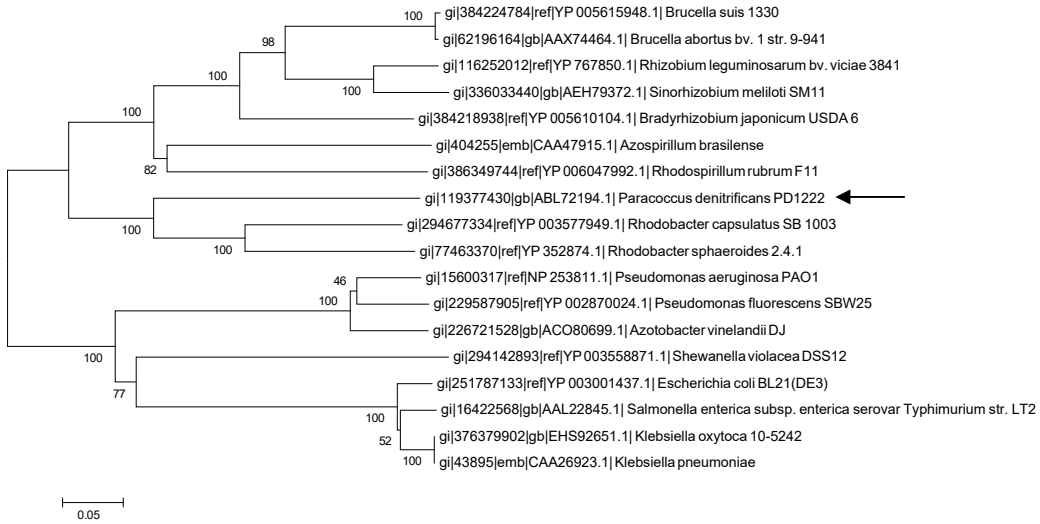
gi|384224784|ref|YP 005615948.1| Brucella suis 1330
gi|62196164|gb|AAX74464.1| Brucella abortus bv. 1 str. 9-941
gi|116252012|ref|YP 767850.1| Rhizobium leguminosarum bv. viciae 3841
gi|336033440|gb|AEH79372.1| Sinorhizobium meliloti SM11
gi|384218938|ref|YP 005610104.1| Bradyrhizobium japonicum USDA 6
gi|404255|emb|CAA47915.1| Azospirillum brasilense
gi|386349744|ref|YP 006047992.1| Rhodospirillum rubrum F11
gi|119377430|gb|ABL72194.1| Paracoccus denitrificans PD1222
gi|294677334|ref|YP 003577949.1| Rhodobacter capsulatus SB 1003
gi|77463370|ref|YP 352874.1| Rhodobacter sphaeroides 2.4.1
gi|15600317|ref|NP 253811.1| Pseudomonas aeruginosa PAO1
gi|229587905|ref|YP 002870024.1| Pseudomonas fluorescens SBW25
gi|226721528|gb|ACO80699.1| Azotobacter vinelandii DJ
gi|294142893|ref|YP 003558871.1| Shewanella violacea DSS12
gi|251787133|ref|YP 003001437.1| Escherichia coli BL21(DE3)
gi|16422568|gb|AAL22845.1| Salmonella enterica subsp. enterica serovar Typhimurium str. LT2
gi|376379902|gb|EHS92651.1| Klebsiella oxytoca 10-5242
gi|43895|emb|CAA26923.1| Klebsiella pneumoniae
0.05

B

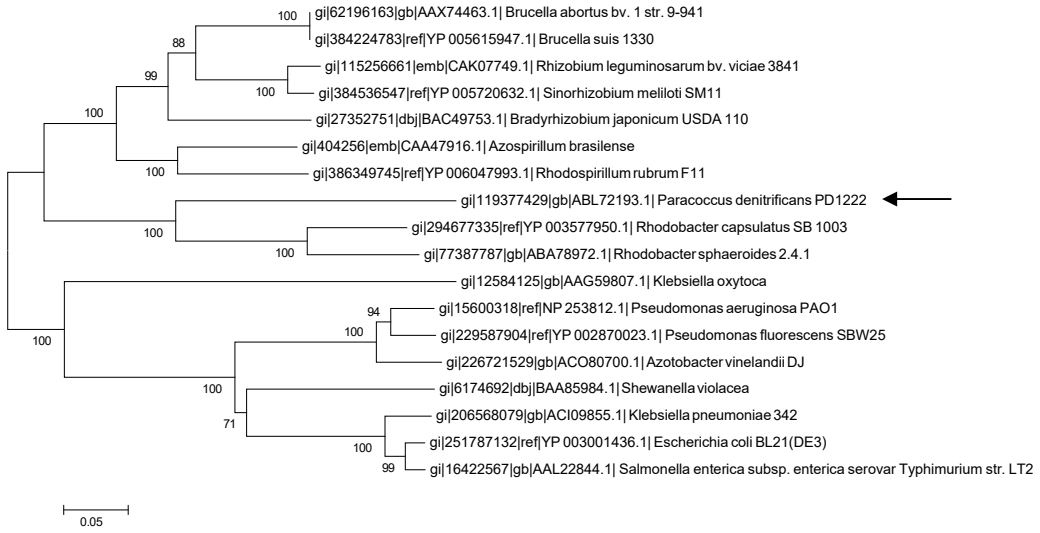
gi|62196163|gb|AAX74463.1| Brucella abortus bv. 1 str. 9-941
gi|384224783|ref|YP 005615947.1| Brucella suis 1330
gi|115256661|emb|CAK07749.1| Rhizobium leguminosarum bv. viciae 3841
gi|384536547|ref|YP 005720632.1| Sinorhizobium meliloti SM11
gi|27352751|dbj|BAC49753.1| Bradyrhizobium japonicum USDA 110
gi|404256|emb|CAA47916.1| Azospirillum brasilense
gi|386349745|ref|YP 006047993.1| Rhodospirillum rubrum F11
gi|119377429|gb|ABL72193.1| Paracoccus denitrificans PD1222
gi|294677335|ref|YP 003577950.1| Rhodobacter capsulatus SB 1003
gi|77387787|gb|ABA78972.1| Rhodobacter sphaeroides 2.4.1
gi|12584125|gb|AAG59807.1| Klebsiella oxytoca
gi|15600318|ref|NP 253812.1| Pseudomonas aeruginosa PAO1
gi|229587904|ref|YP 002870023.1| Pseudomonas fluorescens SBW25
gi|226721529|gb|ACO80700.1| Azotobacter vinelandii DJ
gi|6174692|dbj|BAA85984.1| Shewanella violacea
gi|206568079|gb|ACI09855.1| Klebsiella pneumoniae 342
gi|251787132|ref|YP 003001436.1| Escherichia coli BL21(DE3)
gi|16422567|gb|AAL22844.1| Salmonella enterica subsp. enterica serovar Typhimurium str. LT2
0.05

Figure S1

A

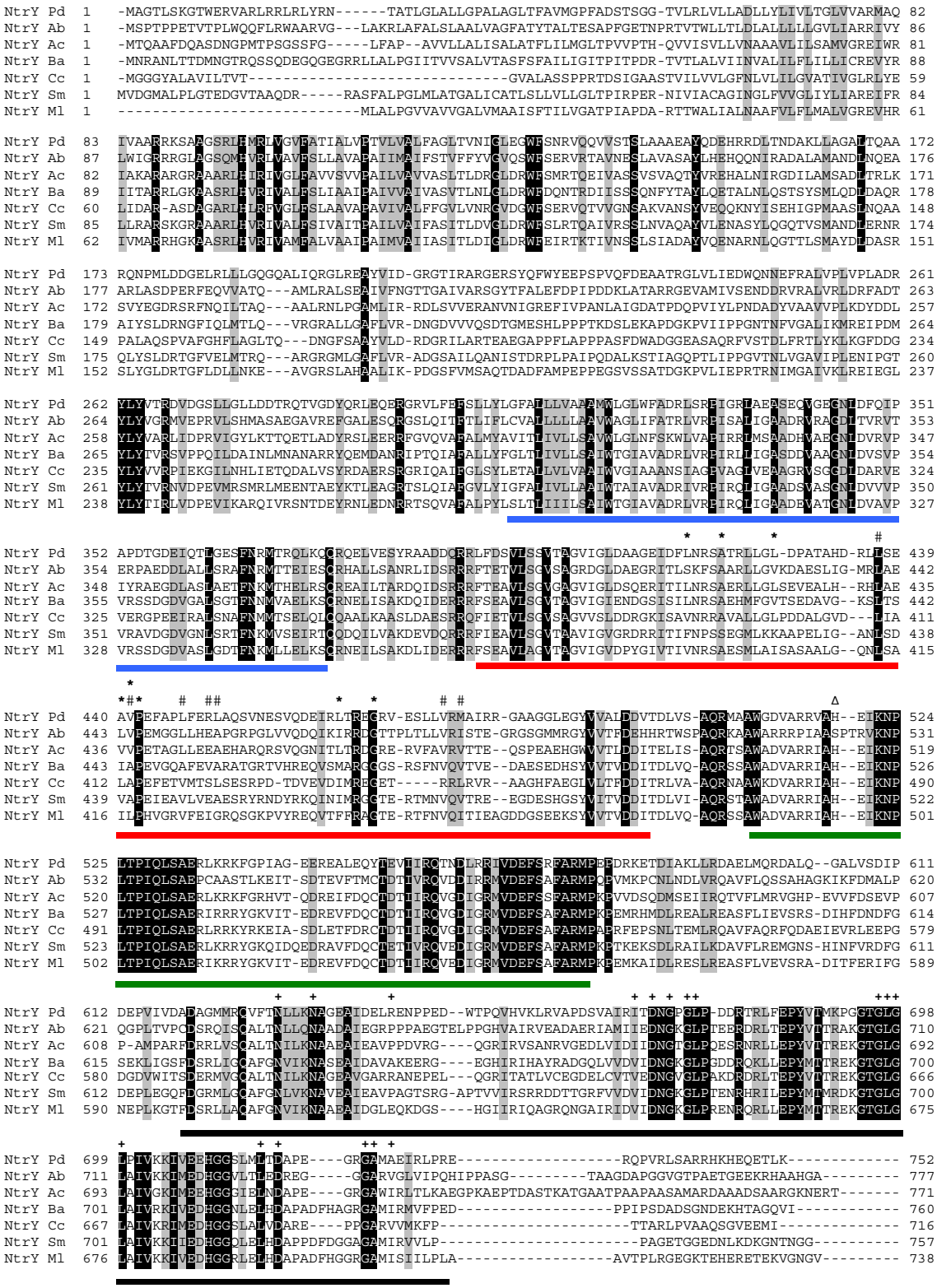

B

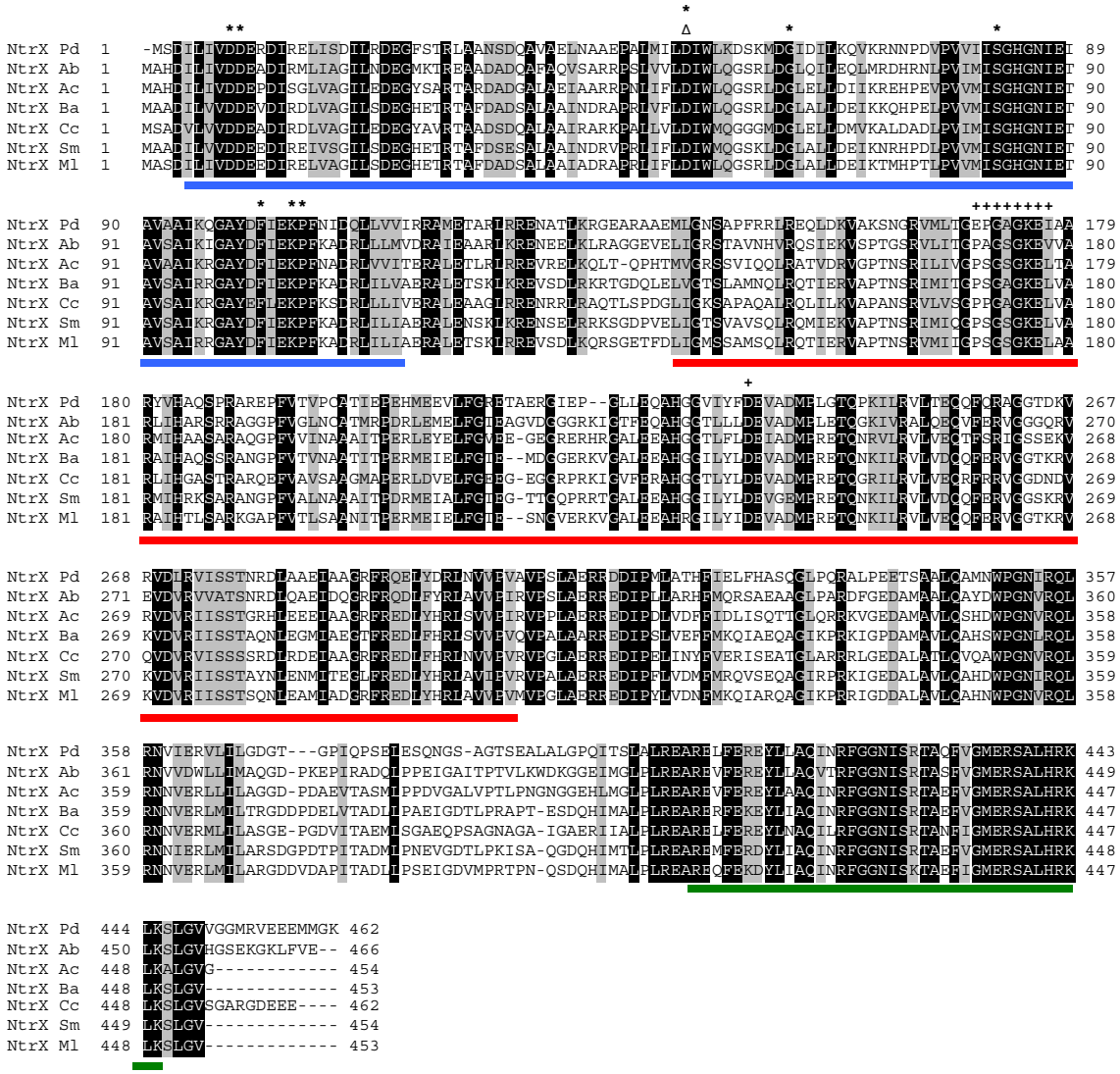

Figure S2

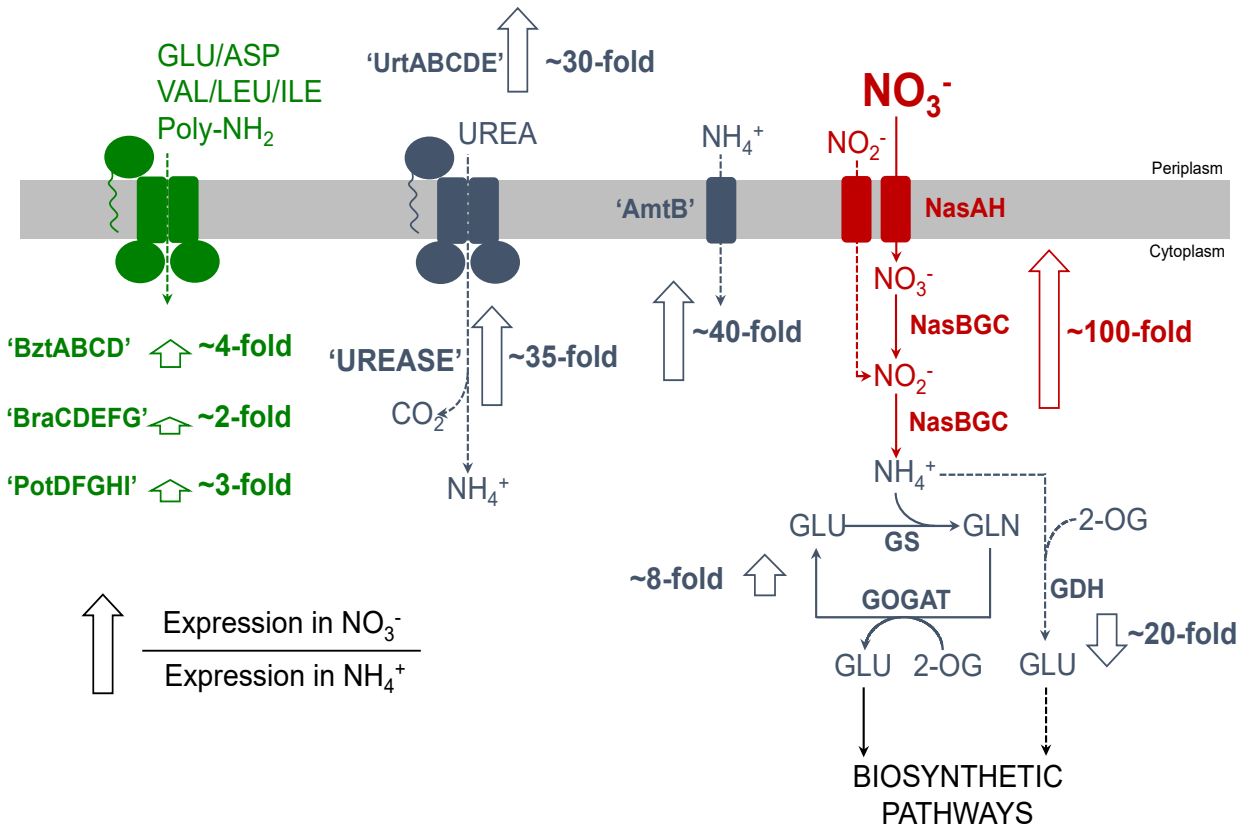
GLU/ASP
VAL/LEU/ILE
Poly-NH2
'UrtABCDE'
~30-fold
UREA
NH4+
NO3-
NO2-
Periplasm
'AmtB'
NasAH
Cytoplasm
NO3-
NasBGC
~100-fold
'BztABCD'
~4-fold
'UREASE'
~35-fold
~40-fold
CO2
NO2-
NasBGC
'BraCDEFG'
~2-fold
NH4+
NH4+
'PotDFGHI'
~3-fold
GLU
GS
GLN
2-OG
~8-fold
GOGAT
GDH
~20-fold
GLU
2-OG
GLU
BIOSYNTHETIC
PATHWAYS
Expression in NO3-
Expression in NH4+

Figure S3

FIGURE LEGENDS

Figure S1. Phylogenetic trees with NtrB (A) and NtrC (B) homologues. The evolutionary history was inferred using the Neighbor-Joining method [11]. The bootstrap consensus tree was inferred from 3000 replicates [12]. Branches corresponding to partitions reproduced in less than 50% bootstrap replicates are collapsed. The percentage of replicate trees in which the associated taxa clustered together in the bootstrap test (3000 replicates) are shown next to the branches [12]. The evolutionary distances were computed using the p-distance method and are in the units of the number of amino acid differences per site. The analysis involved 18 amino acid sequences. All positions containing gaps and missing data were eliminated. There were a total of 330 positions in the final dataset. Evolutionary analyses were conducted in MEGA5 [13]. The *P. denitrificans* sequences are highlighted by arrows.

Figure S2. **Sequence alignment of the two-component regulatory system NtrY (A) and NtrX (B).** Alignment was performed using ClustalW. Identical and similar residues are shaded in black and grey respectively. Regions of selected sequences are highlighted by boxes (located below their respective sequences) and show significant matches with the protein family database (Pfam-A, http://pfam.sanger.ac.uk/) for the following domains: A. HAMP linker domain (blue box), PAS domain involved in many signaling proteins where they are used as a signal sensor domain (red box), phospho-acceptor domain (green box), ATPase domain of histidine kinases (black box). B. Response regulator receiver domain (blue box), sigma54 interaction domain (red box); and helix-turn-helix (HTH) structural motif capable of binding DNA (green box). Asterisks define the position of conserved residues at the active site, triangles indicate the phosphorylation site, crosses define the ATP binding site, and points indicate the heme binding pocket. Pd, *Paracoccus denitrificans* PD1222 (NtrY, gi|119377428 and NtrX, gi|119377427); Ab, *Azospirillum brasilense* Sp245 (NtrY, gi|20451353 and NtrX, gi|119377427); Ac, *Azorhizobium caulinodans* ORS 571 (NtrY, gi|38737 and NtrX, gi|38738); Ba, *Brucella melitensis* biovar Abortus 2308 (NtrY, gi|123754544 and NtrX, gi|82699956); Cc, *Caulobacter crescentus* CB15 (NtrY, gi|16125986 and NtrX, gi|16125987); Sm, *Sinorhizobium meliloti* SM11 (NtrY, gi|336033438 and NtrX,

gi|336033437); Ml, *Mesorhizobium loti* MAFF303099 (NtrY, gi|14021375 and NtrX, gi|14021376).

Figure S3. Schematic overview of the nitrate-regulated systems in *Paracoccus denitrificans*. Transcriptomic data reveal systems that are up-regulated (⇑) or down-regulated (⇓) by nitrate. The fold changes are indicated. Proteomic analysis also corroborated these results.

REFERENCES

1. de Vries, G. E., Harms, N., Hoogendijk, J., and Stouthamer, A.-H. (1989) Isolation and characterization of *Paracoccus denitrifcans* mutants with increased conjugation frequencies and pleiotropic loss of (nGATCn) DNA-modifying property. Arch. Microbiol. **152**, 52-57
2. Luque-Almagro, V. M., Lyall, V. J., Ferguson, S. J., Roldán, M. D., Richardson, D. J., and Gates, A. J. (2013) Nitrogen oxyanion-dependent dissociation of a two-component complex that regulates bacterial nitrate assimilation. J. Biol. Chem. **288**, 29692–29702
3. Sambrook, J., Fritsch, E.F., and Maniatis, T. (1989) Molecular cloning. In A laboratory manual, 2nd edn. New York: Cold Spring Harbor Laboratory, Cold Spring Harbor
4. Figurski, D. H., and Helinski, D. R. (1979) Replication of an origin-containing derivative of plasmid RK2 dependent on a plasmid function provided in trans. *Proc. Natl. Acad. Sci. USA* **76,** 1648–1652
5. Yanisch-Perron, C., Vieira, J., Messing, J. (1985) Improved M13 phage cloning vectors and host strains: nucleotide sequencing of the M13mp18 and pUC9 vectors. Gene **33**, 103-119
6. Simon, R., Priefer, U., and Pühler, A. (1983) A broad host range mobilization system for *in vivo* genetic engineering. Biotechnology **1**, 784–791
7. Gates A. J., Luque-Almagro, V. M., Goddard, A. D., Ferguson, S. J., Roldán, M. D., and Richardson, D. J. (2011) A composite biochemical system for bacterial nitrate and nitrite assimilation as exemplified by *Paracoccus denitrificans.* Biochem. J. **435**, 743-753
8. Schafer A., Tauch A., Jager W., Kalinowski J., Thierbach G., Pühler A. (1994) Small mobilizable multi-purpose cloning vectors derived from the *Escherichia coli* plasmids pK18 and pK19: selection of defined deletions in the chromosome of *Corynebacterium glutamicum*. Gene **145**, 69-73
9. Frigaard, N. U., Li, H., Milks, K. J., and Bryant, D. A. (2004) Nine mutants of *Chlorobium tepidum* each unable to synthesize a different chlorosome protein still assemble functional chlorosomes. J. Bacteriol. **186**, 646–653

10. Spaink, H. P., Wijffelman, C. A., Pees, E., Okker, R. J. H., and Lugtenberg B. J. J. (1987) *Rhizobium* nodulation gene *nodD* as a determinant of host specificity. Nature **328**, 337-340

11. Saitou N. and Nei M. (1987) The neighbor-joining method: A new method for reconstructing phylogenetic trees. Mol. Biol. Evol. **4**, 406-425

12. Felsenstein J. (1985) Confidence limits on phylogenies: An approach using the bootstrap. Evolution **39**, 783-791

13. Tamura K., Peterson D., Peterson N., Stecher G., Nei M., and Kumar S. (2011) MEGA5: molecular evolutionary genetics analysis using maximum likelihood, evolutionary distance, and maximum parsimony methods. Mol. Biol. Evol. **28**, 2731-2739